UNIVERSITY OF CALGARY

Macroscopic quantum effects based on Kerr nonlinearities

by

Tian Wang

A THESIS

SUBMITTED TO THE FACULTY OF GRADUATE STUDIES

IN PARTIAL FULFILLMENT OF THE REQUIREMENTS FOR THE

DEGREE OF MASTER OF SCIENCE

DEPARTMENT OF PHYSICS AND ASTRONOMY

CALGARY, ALBERTA

SEPTEMBER, 2014

Abstract

Glorious victories have been achieved when quantum theory (QT) is applied to microscopic systems. However, although there might be good reasons for us to believe that QT applies at the macroscopic level as well, to give a definite answer "yes" there is still a long journey. If it does apply, a direct result is that it predicts highly counter-intuitive macroscopic quantum superpositions and entanglements, which we never experience in our daily lives.

In this thesis we assume that QT applies to the macroscopic level, and try to find out why we never really observe macroscopic quantum effects. The thesis contains two projects, aiming at two reasons for the above problem. In the first project (Chapter 3 and 4), we show that the required resolution to observe macroscopic quantum effects increases with the size of the system, when both outcome precision and control precision are taken into account. This means that for really large quantum effects we need a very good measuring resolution to observe them, while what we usually do are coarse-grained measurements, whose resolutions are much lower.

In the second project (Chapter 5), we try to deal with decoherence, another obstacle preventing us from observing macroscopic quantum effects. We propose to create and detect strong entanglement of micro-macro and macro-macro beams of photons with very weak cross Kerr nonlinearities that are obtainable by current technology. We analyze the entanglement under environmental decoherence with various methods, and show that strong entanglement can still be created and detected under decoherence.

We hope that the above results will help to push the boundary of the realm of QT towards the macroscopic level.

List of papers published, submitted or to be submitted

T. Wang, R. Ghobadi, S. Raeisi, C. Simon, "*Precision requirements for observing macroscopic quantum effects*" Phys. Rev. A 88, 062114 (2013).

H. Lau, Z. Duton **T. Wang**, C. Simon, "*Proposal for the Creation and Optical Detection of Spin Cat States in Bose-Einstein Condensates*" Phys. Rev. Lett. 113 (9), 090401.

T. Wang, ... C. Simon, "*Strong entanglement between Macroscopic beams via weak Kerr nonlinearities*" In preparation.

T. Wang, D. Hobill, "*Is pointer basis selected by the environment?*" In preparation.

T. Wang, R. Ghobadi, S. Raeisi, C. Simon, "*Demonstrating macroscopic entanglement based on Kerr non-linearities requires extreme phase resolution*", Proceeding of Frontiers in Optics/Laser Science 2013

Acknowledgements

First of all, I would like to thank my supervisor, Prof. Christoph Simon, for his encouragement, support, and patient guidance. The two years in Christoph's group is the happiest time in my life. When I came here, I had no basics of quantum optics at all, and had to spend months just in learning. Yet Christoph was always patient and supportive, keeping encouraging me, even though I was slow in the beginning. During these two years I not only harvested knowledge and skills to conduct research, but also a deeper understanding of myself. Firstly, I regain my confidence in physics. I was regarded as gifted in Arts and Humanities, yet I chose physics as my major, since I believe that only physics can answer the ultimate questions of our world. However, I was not sure whether I am suitable for a career as a physicist. In my undergrad I actually spent 90% of my time in Arts and Humanities, as I did not think I could do anything meaningful in physics at that time, while Arts and Humanities had been proven to be a better stage for me. I had seriously considered switching into Arts and Humanities many times, since despite my great curiosity I had never shown any success in real physics research. It was in Christoph's group that I finally stopped this idea, as I convinced myself that I could do good physics. Under Christoph's guidance, I am able to produce meaningful results with my relatively limited knowledge. I realized that research in physics is not that enigmatic. As he put it, the key factors for success in physic is a certain amount of talent and strong motivation, and I have both of them. Secondly, I realized that I love physics more than I thought. As a curiosity driven person, I always thought that I was only interested in those fundamental questions such as the origin of universe, while have little interest in applied science. I still remember the tortures in my first few group meetings when listening to inscrutable discussions about quantum memory, with ample of jargon like "EIT" "AFC" haunted around my ears. However, as my knowledge accumulates, I began to realize that doing something that can be realized in experiments with potential application is also

cool. The main reason that I disliked it before is simply that I do not understand it. Now I am willing to work on those technical problems, which would provide me the knowledge and skills that would be helpful for future fundamental research. Moreover, I found that I actually enjoy doing calculations. I always thought that I enjoy philosophical thinking such as analyzing concepts (which I do) while hate doing complicated calculations. But during these two years I found that it is not true. Calculations in research are completely different with that in exercises; each step ahead in the former represents a small yet sometimes meaningful progress in the human understanding of nature. I especially enjoy the excitements when a seemingly formidable calculation was done by reasonable approximations and clever tricks, and gives out a simple analytic expression that matches our intuition. Finally, I found out that I could also be very hardworking. I can spend days and nights in Arts and Humanities, but that is not what I was supposed to do. During my 16 years of fighting with the education system in China, I was by no means a hard working student. When I was young I could always spend little time to learn everything by myself very efficiently and get a good mark, while sparing time for what I love. However, as the content became more difficult, I found out that when I really need to be more focused, I could hardly join my peers who work ridiculously hard: I lost the ability to be hardworking. Fortunately here I found out that I magically regain this ability– when I really focus on my research I can consecutively work 12 hours a day with high efficiency. Thanks to these two years' experience I am now confident enough to stick to and fight for my childhood dream–explore our mysterious nature.

I also like to thank Prof. David Hobill. I took two courses with David, in both of which I was the student with most questions. David always answers my questions clearly and patiently, both in and after class. I enjoyed discussing with David on various interesting topics of physics, learning from his broad knowledge.

I would like to thank my friends Honwai, Khabat, Farid, Hamid, Mohammad, Abhirup, Mark, Varun, Ish, Adarsh, Farokh and Raju, for the help in both physics and life.

Finally, I would like to thank my family, especially my wife Shuai, for all their support and encouragement during this two years.

Table of Contents

Abstract . . . i
List of papers published, submitted or to be submitted . . . ii
Acknowledgements . . . iii
Table of Contents . . . vi
List of Tables . . . viii
List of Figures . . . ix
List of Symbols . . . xii
1 Introduction: why is it hard to observe Schrodinger's Cat . . . 1
1.1 No interference experiments . . . 2
1.2 Decoherence . . . 3
1.3 Measurement precision . . . 4
1.4 The structure of this thesis . . . 5
Bibliography . . . 6
2 Basics of quantum optics and quantum information . . . 7
2.1 Coherent states and Cat states . . . 7
2.1.1 Coherent states . . . 7
2.1.2 Cat states . . . 8
2.2 Beam splitter model of quantum loss . . . 9
2.3 Kerr effect . . . 10
2.4 Quantum entanglement . . . 10
Bibliography . . . 12
3 Demonstrating macroscopic entanglement based on Kerr non-linearities requires extreme phase resolution . . . 13
3.1 Preface . . . 13
3.2 Introduction . . . 14
3.3 Coarse-grained measurement scheme . . . 16
3.4 Extremely high requirement of nonlinear phase control . . . 18
3.4.1 Rotation and deformation effects of cat state evolution in Kerr medium 18
3.4.2 Characteristic phase when the cat state "collapse due to phase error . 25
3.5 conclusion . . . 27
Bibliography . . . 29
4 Precision requirements for observing macroscopic quantum effects . . . 31
4.1 Preface . . . 31
4.2 Introduction . . . 31
4.3 Macroscopic superpositions: requirement for high outcome precision . . . 33
4.4 Nonlinear rotations of coherent-state qubits: requirement for high control precision . . . 36
4.5 Macroscopic entanglement . . . 42
4.6 Conjecture and discussion . . . 43
Bibliography . . . 46
5 Strong entanglement between macroscopic beams via weak cross Kerr-nonlinearties 48
5.1 Introduction . . . 48

5.2 Strong entanglement 49
5.3 Robust under Decoherence 53
5.4 Appendix 59
5.4.1 Derivation of the purity 59
5.4.2 Proof of the witness 61
5.4.3 Calculation of the value of the witness under decoherence 62
Bibliography 65
6 Conclusion and outlook 67
Bibliography 70

List of Tables

2.1 comparison of entanglement monotones 11

List of Figures and Illustrations

1.1 Schrodinger's Cat 2
1.2 Electron double slits experiment 3

3.1 **Scheme to observe macroscopic entanglement with very coarse-grained measurements.** The coherent state $|\sqrt{2}\alpha\rangle$ (with $\alpha \gg 1$) is transformed into a macroscopic superposition of coherent states Eq. (3.2) using a Kerr non-linear operation (KNL). The superposition is transformed into a maximally entangled state of coherent state qubits Eq. (3.3) using a beam splitter. General single-qubit rotations (SQR) can be implemented using the Kerr nonlinearity following Ref. [16]. Detection in the coherent state qubit basis is done via the displacement of $D(\alpha)$, followed by detectors that only need to distinguish the bright state $|\sqrt{2}\alpha\rangle$ from the vacuum, as shown in Fig. 3.5. This setup would in principle allow the observation of Bell inequality violations (for example), thus demonstrating macroscopic entanglement. 17
3.2 **Q function evolution of the cat states with mean photon number N=16, 64, 256 in the Kerr medium.**
The Q function of ideal cat state is two Gaussian packets. As the phase error ϕ increases, the two components of the cat state get deformed. When ϕ reaches the characteristic phase $\phi_c(N) = \frac{\pi}{4\sqrt{N}}$ Eq. (3.4.2), the two components completely merge with each and the cat state "collapses. From the picture we can see that the cat state collapses more and more quickly with increasing mean photon number N. When $\phi = 0.031\frac{\pi}{2}$, the characteristic phase of N=256 cat state, the two components of N=16 cat state is still distinguishable, while the two components of N=64 cat state already begins to merge, and for N=256 cat state, the two components are evenly distributed in the whole phase, which indicates the cat state collapse. 20
3.3 **Q function evolution of the cat states with mean photon number N=64 with H_{ROT} and the Kerr Hamiltonian H_{KNL}.** It could be seen that the rotation effect of the Kerr evolution has angular speed that is the same with the the speed of the rotation proportional to the mean photon number N. 21
3.4 **Fidelity $F(\phi)$ of the state $|\psi_\phi\rangle$ of Eq. (3.5) relative to the ideal state $|\psi_0\rangle$ of Eq. (3.2) for different values of N.** $F(\phi)$ is a function of the non-linear phase errorϕ. The curves correspond to mean photon numbers $N = 2\alpha^2$ equal to 16, 64 and 256 from top to bottom. The fidelity decays faster and faster as the mean number of photons increases. 23
3.5 **Overlap $F_d(\phi)$ illustrating the deformation effect in the Kerr medium due to the phase error.** $F_d(\phi)$ is a function of ϕ which measures the non-linear phase error. The curves correspond to mean photon numbers $N = 2\alpha^2$ equal to 16, 64 and 256 from top to bottom. The fidelity decays faster and faster as the mean number of photons increases. 24

3.6 **The complete deformation would make the scheme unsuccessful.** The deformation due to the phase error, which increases drastically with increasing photon numbers, makes the above scheme impossible. This is because the coarse grained measurement relies on displacing the cat state in the phase space, making the difference of the mean photon number of the two components very large so that a very coarse grained photon number measurement is able to differentiate them, as shown in the upper pictures. This scheme still hold when each component of the cat state is a little deformed, since the difference of mean photon number is still very large after displacement. However, if the two components completely merge with each other and get evenly distributed in the phase space, the mean photon number difference would become zero, thus the coarse grained measurement ceases to work . . 26

4.1 Probability of outcomes for measurements of the $\hat{p}$ quadrature for the superposition state $|\alpha_+\rangle$ and the mixed state of Eq. (4.2) for $\alpha = 2$ (left) and $\alpha = 16$ (right). The oscillatory structure that distinguishes the two distributions becomes harder to resolve as α increases, see also Eqs. (4.4) and (4.5). 35

4.2 Outcome distributions for measurements of the $\hat{x}$ quadrature for the states $|\alpha\rangle$ (solid) and $|-\alpha\rangle$ (dashed) for $\alpha = 8$. For large enough α, the two states can be distinguished by a very coarse measurement. Positive values (red) of $\hat{x}$ can be assigned to $|\alpha\rangle$ and negative values (blue) to $|-\alpha\rangle$. The overlap between the two distributions, and thus the error of this measurement scheme, is negligible. 36

4.3 The $\hat{x}$ quadrature distributions for the states $|\alpha_+\rangle = \frac{1}{\sqrt{2}}(|\alpha\rangle + i|-\alpha\rangle$ (top left) and $|\alpha_-\rangle = \frac{1}{\sqrt{2}}(i|\alpha\rangle + |-\alpha\rangle$ (bottom left) are identical. However, application of the Kerr rotation Eq. (4.8) transforms $|\alpha_+\rangle$ into $|\alpha\rangle$ (top right) and $|\alpha_-\rangle$ into $|-\alpha\rangle$ (bottom right). These states can now be distinguished by a coarse measurement as in Fig. 4.2. 38

4.4 Outcome distributions for $\hat{x}$ quadrature measurements for the states $C_\sigma(|\alpha\rangle\langle\alpha|)$ (solid) and $C_\sigma(|-\alpha\rangle\langle-\alpha|)$ (dashed) that are created from the states $|\alpha_+\rangle$ and $|\alpha_-\rangle$ by a Kerr rotation with Gaussian phase uncertainty σ, see Eq. (4.9). We show the case $N = \alpha^2 = 4$ on the left and $N = 36$ on the right, with σ increasing from top to bottom. One sees that the distributions overlap much faster for greater N, leading to errors in the σ_y measurement of Fig. 4.3, see also Fig. 4.2. For large enough σ it becomes impossible to distinguish the two states. 40

4.5 (a) The bit-flip error ϵ in the σ_y measurement of Fig. 4.3 as a function of the Kerr phase uncertainty σ, for the cases $N = \alpha^2 = 4, 16, 64$ from bottom to top. One sees that ϵ approaches $\frac{1}{2}$ for increasing σ, and this happens faster for greater N. The log-log plot in the inset shows that the value of σ for which $\epsilon = \frac{1}{4}$ (i.e. half its asymptotic value) scales like $\frac{1}{N}$, as expected from the analytical argument given in the text. (b) Expectation value of the entanglement witness W of Eq. (4.12) for the state of Eq. (4.11), for $N = \alpha^2 = 4, 16, 64$ from top to bottom. For increasing σ the value of W approaches 1 (the bound for separable states), due to the bit-flip errors in the σ_y measurement shown in (a). This happens faster for greater values of N. . 41

5.1 Scheme to create and detect macroscopic entanglement 49
5.2 The structure of the state 50
5.3 Von Neumann Entropy for symmetric (lower, $|\alpha| = |\beta| = 5$) and asymmetric (upper, $|\alpha| = 5, |\beta| = 40$) cases. 52
5.4 $D(\rho)$ (red) and $W(\rho)/2$ with no loss (blue) as the function of the size of the system a for $10^{-3} rad$ cross Kerr phase shift. It can be seen that for $a = 1000$ the entanglement is about 2000 dimensions. Moreover, for $a < 200$ our witness matches the dimension of entanglement very well. 54
5.5 Logarithmic Negativity (dotted) and witness (continuous) as a function of phase shift θ for $|\alpha| = 5, |\beta| = 40$ with various loss rate. The loss rate is $0, 1\%, 5\%, 10\%, 20\%, 40\%, 50\%$ from top to bottom. 55
5.6 Witness as a function of phase shift θ for $|\alpha| = 5, |\beta| = 1000$ with various loss rate.The loss rate is $0, 1\%, 5\%, 10\%, 20\%, 40\%, 50\%$ from top to bottom. It can be seen that the maximum does not change compared to the previous case , however the θ to obtain maximum is much smaller. With 5% loss the maximum is 2.1 at $\theta = 4 * 10^{-4}$. 56
5.7 Witness as a function of $|\alpha|$ and θ when we fix $|\beta| = 1000$ with 10% loss. It can be seen that even though $|\alpha|$ rises to 1000, W is still about 1.6. 59

List of Symbols, Abbreviations and Nomenclature

Symbol	Definition
U of C	University of Calgary
QT	Quantum Theory
LOCC	Local operation and classical communication
KNL	Kerr nonlinearities
AITF	Alberta Innovation Technology Future
NSERC	The Natural Sciences and Engineering Research Council of Canada
QED	Quantum Electrodynamics
QND	Quantum Non-demolition
BEC	Bose Einstein Condensate

Chapter 1

Introduction: why is it hard to observe Schrodinger's Cat

Glorious victories have been achieved when quantum theory (QT) is applied to microscopic systems. Quantum superposition and entanglement, the most striking features of QT that arise from its linear structure, have been verified experimentally in various systems. The electron double slit experiment, the common topic of the first chapter of quantum mechanics textbooks, has been realized in 1989 [4], and was voted as the most beautiful physics experiment [5]. There is no doubt that QT correctly describes the microscopic world.

However, although there might be good reasons for us to believe that QT applies at macroscopic level as well, to give a definite answer "yes" there is still a long journey. The most famous counter example is the Schrodinger's cat gedanken experiment, raised by Schrodinger in 1935. The main idea is very simple.

$$\frac{1}{\sqrt{2}}(|0\rangle + |1\rangle)|A\rangle \rightarrow \frac{1}{\sqrt{2}}(|0\rangle|D\rangle + |1\rangle|A\rangle)$$

A quantum system (such as an atom in this case), can be in superposition of two different states (decayed $|0\rangle$and not decayed states $|1\rangle$). These two different states would interact with the macroscopic object (a cat) differently (decayed atom would kill the cat, not decayed would not). After the interaction, the global system (the cat and the atom) would be in a superposition of two states: decayed atom with a dead cat $|0\rangle|D\rangle$, and non-decayed atom with a alive cat $|1\rangle|A\rangle$. In other words, the atomic state is entangled with the cat state. If we put this atom and the poor cat in a black box, according to QT, before opening the box to do the measurement, the global system would remain in superposition (entangled). However, how can a cat be in a superposition of dead and alive states? If so, can it be ever

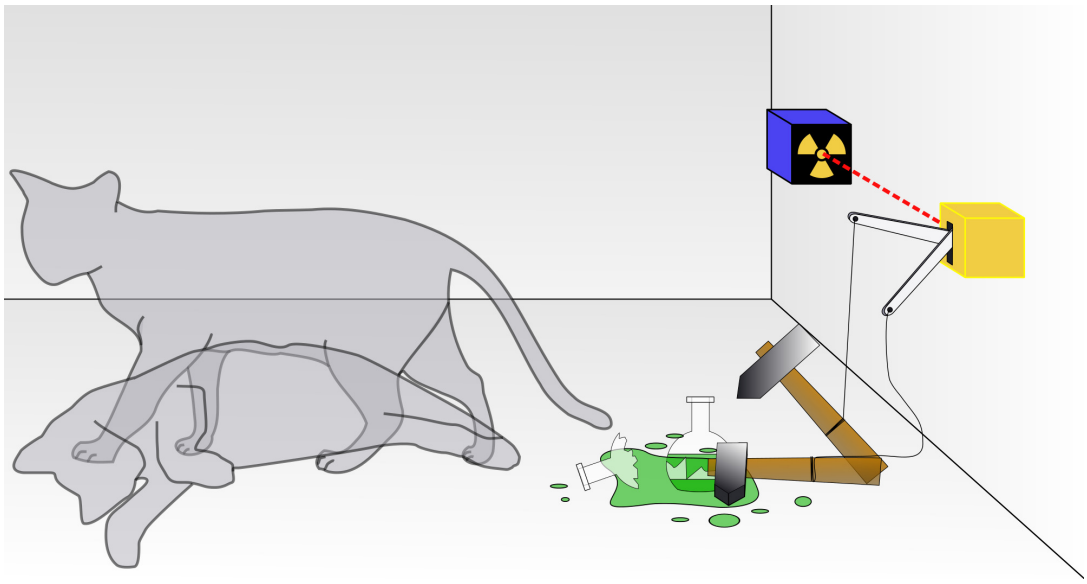

Figure 1.1: Schrodinger's Cat

observed?

Obviously, no one has ever experienced a macro system being in a superposition of two different states, such as a cat being dead and alive and a desk being here and there. Why is this the case? This is a common question raised in many papers and textbooks when talking about foundational problems of QT. In my opinion, there are mainly three reasons.

1.1 No interference experiments

The most direct answer to the questions why no one experienced a desk in superposition of being two different positions, is the fact that no one has ever done proper interference experiments to observe such quantum superposition. As we know, quantum superposition is a statistical effect, which means that to observe it one has to do many rounds of experiments and look at the statistics. We can never verify that something is in superposition of two different states by a single shot. In electron double slit case [4], we have to send a lot of electrons to the slits and look at the pattern on the screen behind. If there is interference fringe we can infer that the electron was in a superposition of passing through each slit. For

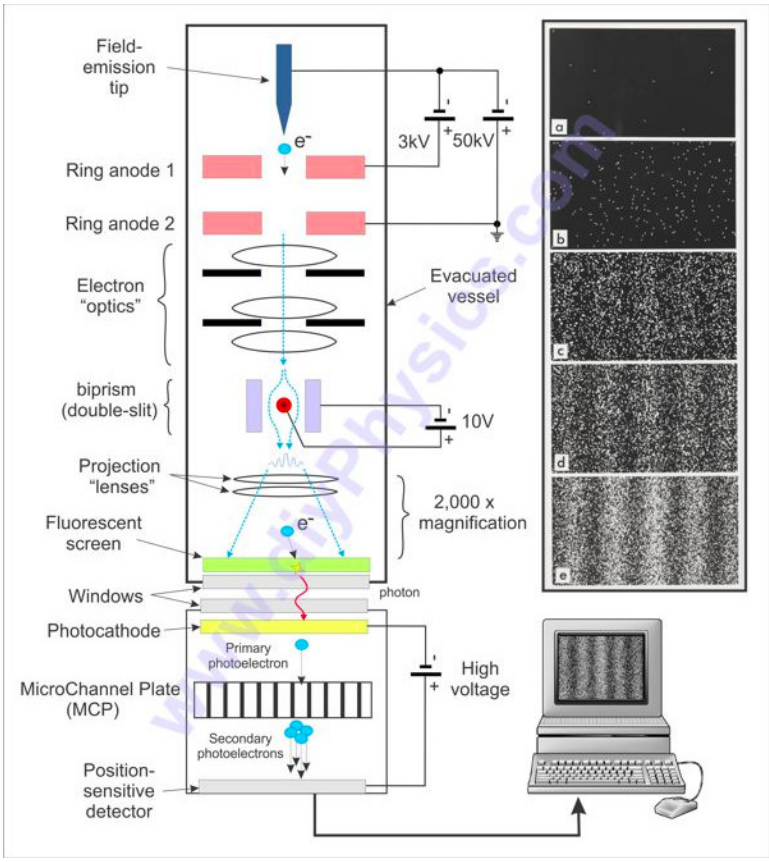

Figure 1.2: Electron double slits experiment

the same reasons, to verify the desk is in a superposition of being two different locations, one also needs to do proper interference experiments. However in our daily experiences, no one has ever tried to do such experiments. In my opinion, this is the most direct reason. Although it is true that for macroscopic systems such interference experiments are hard to realize, due to decoherence and high requirement for measurement resolution, as discussed later, yet a lot of literature never even mentioned that interference experiments are prerequisite for observing quantum effects.

1.2 Decoherence

The second reason is decoherence [1], the common answer to this problem given in the literature. The main idea is that the global system is actually also interacting with the environ-

ment, bringing the environment into entanglement. The two macroscopic states ($\{|A\rangle, |D\rangle\}$) interact with the environment differently and the corresponding two environmental states ($\{|E_0\rangle, |E_1\rangle\}$) become orthogonal very quickly.

$$\frac{1}{\sqrt{2}}(|0\rangle + |1\rangle)|A\rangle|E_0\rangle \rightarrow \frac{1}{\sqrt{2}}(|0\rangle|D\rangle + |1\rangle|A\rangle)|E_0\rangle \rightarrow \frac{1}{\sqrt{2}}(|0\rangle|D\rangle|E_0\rangle + |1\rangle|A\rangle|E_1\rangle)$$

As we cannot monitor the state of the environment, we have to average it out. The reduced density matrix of the global system becomes:

$$\rho_{sa} = Tr_e(\rho_{sae}) = \frac{1}{2}(\,|\,0, D\rangle\langle 0, D| + |1, A\rangle\langle 1, A|)$$

The off-diagonal terms which characterize the quantum coherence of $\{|0, D\rangle, |1, A\rangle\}$ vanish, which means that the quantum coherence is lost and the state becomes a statistical mixture (there is no interference pattern).

Decoherence is one of the main obstacles in quantum information science. In general, the larger the system is, the stronger it interacts with the environment, and the more sensitive it is to decoherence. Thus the problem of observing macroscopic quantum effects becomes how to create and detect macroscopic quantum effects before they become decohered. The second project in this thesis is to create and detect macroscopic quantum entanglement that is robust under decoherence via optical Kerr effect, see Chapter 5 for detail.

1.3 Measurement precision

The third reason for not observing macroscopic quantum effect is that the measurement precision may not be high enough [6] [9]. To detect macroscopic quantum effects, there are certain requirements in measurement precision. If such requirements are not satisfied, even if we have macroscopic quantum superposition or entanglement, the statistics we obtain may be similar to classical mixtures. It has been conjectured that the requirement in measurement precision would increase as the size of the system increases. Chapter 4 deals with this issue in detail.

1.4 The structure of this thesis

This thesis concentrates on the topic how to create and detect macroscopic quantum effect. Our goal is to push the boundary of the realm of QT towards macroscopic level. We mainly focus on quantum optical systems, with the help of optical Kerr effect. The thesis contains two projects, aiming at the second and third points above respectively. The thesis is organized as follow. Chapter 2 reviews the basis of quantum optics and quantum information. Chapter 3 and Chapter 4 analyzed the measurement precision required to detect macroscopic quantum effects, reconciled contradictory results from two PRL papers, generalized the concept of coarse measurements, and revealed that it is increasingly difficult for coarse measurement to reveal macroscopic quantum effect with increasing size of the system. Chapter 5 analyzed a new class of macroscopic entangled states generated by weak cross Kerr phase shift. We tried various methods, including developing our own entanglement witness, to quantify and analyze the entanglement, and verified that such entanglement is robust under decoherence.

Bibliography

[1] T. Wang, R. Ghobadi, S. Raeisi, and C. Simon, Phys. Rev. A 88, 062114 (2013).

[2] W.H. Zurek, Rev. Mod. Phys. **75**, 715 (2003).

[3] S. Raeisi, P. Sekatski, and C. Simon, Phys. Rev. Lett. **107**,

[4] http://www.hitachi.com/rd/portal/research/em/doubleslit.html

[5] http://physicsworld.com/cws/article/print/2002/sep/01/the-most-beautiful-experiment

Chapter 2

Basics of quantum optics and quantum information

2.1 Coherent states and Cat states

2.1.1 Coherent states

Coherent states $|\alpha\rangle$ are usually considered as the most "classical" quantum states in quantum optics[1][2][3]. One of the reasons is that the expectation value of the electric field has the form of the classical expression. Another reason is that the fluctuations in the electric field operator are the same as for a vacuum states. Moreover, the states become well localized in phase with increasing average photon number. The laser pulse generated in experiments can usually be considered as a coherent state. It is defined as the eigenstate of the annihilation operator $\hat{a}|\alpha\rangle = \alpha|\alpha\rangle$. Expended in the fock basis,

$$|\alpha\rangle = e^{-|\alpha^2|} \sum_{n=0}^{\infty} \frac{\alpha^n}{\sqrt{n!}} |n\rangle$$

Let us consider the expectation value of the electric field operator $\hat{E}(r,t) = i\left(\frac{\hbar\omega}{2\epsilon_0 V}\right)^{\frac{1}{2}} [\hat{a}e^{i(kr-\omega t)} - \hat{a}^\dagger e^{-i(kr-\omega t)}]$, we obtain

$$\langle\alpha|\hat{E}(r,t)|\alpha\rangle \quad = 2|\alpha|\left(\frac{\hbar\omega}{2\epsilon_0 V}\right)^{\frac{1}{2}} sin(\omega t - kr - \theta)$$

where $\alpha = |\alpha|e^{i\theta}$. Such an expectation value looks like a classical field. The fluctuations in $\hat{E}(r,t)$ is$\Delta E = \left(\frac{\hbar\omega}{2\epsilon_0 V}\right)^{\frac{1}{2}}$, identical to those for a vacuum state.

The fluctuations in photon number $\hat{n}$ is $\Delta n = \sqrt{\langle\hat{n}^2\rangle - \langle\hat{n}\rangle^2} = \sqrt{\bar{n}}$

which is the characteristic of the Poisson distribution. In fact, the probability P_n of detecting n photons is

$$P_n \quad = \quad |\langle n|\alpha\rangle|^2 = e^{-|\alpha|^2} \frac{|\alpha|^{2n}}{n!} = e^{-\bar{n}} \frac{\bar{n}^n}{n!}$$

which is a Poisson distribution with a mean of $\bar{n}$.

Coherent states can also be defined as displaced vacuum states. The displacement operator is defined as

$$\hat{D}(\alpha) = exp(\alpha\hat{a}^\dagger - \alpha^\star\hat{a})$$

and the coherent states are given as

$$|\alpha\rangle = \hat{D}(\alpha)|0\rangle$$

The reason why it is named "displaced operator" it that the quasi-probabilistic distributions of the states would be displaced in phase space. This operator will be highly useful later.

2.1.2 Cat states

In analogy to superposition of two different classical states (dead and alive cats), Schrodinger's cat states in quantum optics, often abbreviated as "cat states", are the superposition of different coherent states, especially when they are quasi-orthogonal. One of the common cat states is a superposition of two coherent states with opposite phases, which can be generated via self Kerr effect (see below).

$$\frac{1}{\sqrt{2}}(|\alpha\rangle + i|-\alpha\rangle)$$

Actually, as long as α is large enough, coherent states with small phase difference can also be quasi-orthogonal. For instance, for a being a large real number

$$|\langle a|ae^{-i\phi}\rangle|^2 = e^{-2a^2(1-cos(i\phi))}e^{-(a\phi)^2}$$

This indicates that when $a\phi > 1$

$$\frac{1}{\sqrt{2}}(|a\rangle + e^{i\theta}|ae^{-i\phi}\rangle)$$

is also a good cat states ($e^{i\theta}$ is the general quantum phase). This result would be useful in Chapter 5 of this thesis.

2.2 Beam splitter model of quantum loss

In quantum optics, the main source of decoherence is photon loss. This is because that in realistic conditions not all photons can really reach the next step, such as the detectors. The beam splitter model of quantum loss provides the means to determine the quantum state after it has undergone loss. The model consists of replacing the lossy channel with a beam splitter that has the same transmission rate and with the vacuum state entering its other channel. The reflected mode of the beam splitter is assumed to be lost.

It can be shown that a fock state passing through a beam splitter could be represented as

$$\hat{B}|n,0\rangle \rightarrow \sum_{n=0}^{\infty} A_{nk}|n-k,k\rangle$$

where

$$A_{nk} = \sqrt{\begin{pmatrix} n \\ k \end{pmatrix}} t^{n-k} r^k$$

here t^2 and r^2 is the transimisitivity and reflectivity respectively.

Thus a quantum state with a density matrix

$$\rho = \sum_{m,n=0}^{\infty} \rho_{mn}|m\rangle\langle n|$$

passing through a beam splitter will generate a two mode density matrix

$$\rho = \sum_{m,n=0}^{\infty} \sum_{j=0}^{m} \sum_{k=0}^{n} \rho_{mn} A_{mj} A_{nk} |m-j,j\rangle\langle n-k,k|$$

By taking the partial trace over the reflected mode, we obtain the density matrix of the transmitted mode:

$$\rho_{out} = Tr_2\rho = \sum_{m,n=0}^{\infty} \sum_{k=0}^{min(m,n)} \rho_{mn} A_{mk} A_{nk} |m-k\rangle\langle n-k|$$

The above transformation is called the generalized Bernoulli transformation.

It can also be shown that a coherent state $|\alpha\rangle$, after propagation through a loss channel with transmissivity t^2, becomes $|t\alpha\rangle$. This result will be highly useful in the second project of this thesis.

2.3 Kerr effect

The Kerr effect is a change in the refractive index of a material in response to an applied electric field. It is one of the most frequently used nonlinear effects in quantum optics [7]. The Kerr effect can be divided into the self Kerr effect, in which the refractive index is changed due to the response of the incoming field itself, and the cross Kerr effect, in which the refractive index is changed due to the response of the another field. The interaction Hamiltonian for the self Kerr non-linearity is

$$H_{sk} = K(a^\dagger a)^2, \tag{2.1}$$

and for the cross Kerr non-linearity is

$$H_{ck} = K a_1^\dagger a_1 a_2^\dagger a_2. \tag{2.2}$$

More details of Kerr effect will be provided in Chapter 3,4 and 5.

2.4 Quantum entanglement

Quantum Entanglement is one of the most fascinating and counter-intuitive aspects of quantum theory. A state of a bipartite system is called entangled if it cannot be written as a direct product of two states from the two subsystem Hilbert spaces. For mixed states, entangled states are those that could not be written as a convex combination of product of density matrix from the two subsystem Hilbert spaces.

How to quantify entanglement under various conditions is still an open question. To quantify entanglement one needs to use entanglement monotones, which do not increase under local operation and classical communication (LOCC), since LOCC cannot create entanglement. In Table 2.1 we compares several entanglement monotones that are often used[4, 6, 5].

Unfortunately, in the second project we need to quantify non-Gaussian continuous variable bipartite large entanglements, where none of the above entanglement monotones really

Table 2.1: comparison of entanglement monotones

Entanglement monotones	mixture	continuous variable	non-Gaussian states	experimentally detectable
von Neumman entropy	no	no	yes	hard
logarithmic negativity	yes	no	yes	hard
covariance matrix method	yes	yes	no	easy
concurrence	yes	no	yes	easy
(inverse) quantum purity	no	sometimes yes	yes	hard

apply. So we develop our own entanglement witness based on the structure of our state. An entanglement witness is a functional which distinguishes a specific entangled state from separable ones. When it is above some specific value, it means the states are not separable, and thus the entanglement could be shown.

Bibliography

[1] Gerry C.C., Knight P.L., Introductory quantum optics (CUP 2004).

[2] A. Lvovsky, Lecture notes in quantum and nonlinear optics.

[3] Scully M.O., Zubairy M.S. Quantum optics (CUP, 1997).

[4] Scott Hill, William K. Wootters, Phys.Rev.Lett.78:5022-5025,1997.

[5] R. Simon, Phys. Rev. Lett. 84, 2726 (2000).

[6] M.B. Plenio, Phys. Rev. Lett. 95, 090503 (2005).

[7] Masamoto Takatsuji, Phys. Rev. 155, 980 (1967).

Chapter 3

Demonstrating macroscopic entanglement based on Kerr non-linearities requires extreme phase resolution

3.1 Preface

It has recently been conjectured that detecting quantum effects such as superposition and entanglement for macroscopic systems always requires a measurement precision that increases with the size of the system. We analyze this conjecture for the case of macroscopic superposition and entanglement of coherent states. Measurements with low outcome resolution can be sufficient if Kerr or higher-order nonlinearities are available for basis rotation. However, the phase of this non-linear rotation has to be controlled with a precision that increases with the size of the system. This suggests a refined conjecture that either the outcome precision or the control precision of the measurements has to increase with the size of the system.

This chapter is based on one proceeding "*Demonstrating macroscopic entanglement based on Kerr non-linearities requires extreme phase resolution*", Frontiers in Optics 2013, and an unpublished paper with the same title. It could be seen as the preliminary result for the topic "can coarse-grained measurement reveal macroscopic quantum effects", to be continued in the next chapter. Actually we were about to submit the paper, then we found out a better approach for this topic, which is presented in the next chapter. This chapter mainly discusses the precision requirement to create macroscopic quantum effects, while next chapter discusses the precision requirement to observe macroscopic quantum effects. My contribution is that I did the calculations, drew the graphs and helped write the paper.

3.2 Introduction

What does it take to observe quantum effects such as superposition and entanglement for macroscopic systems? It is nowadays well understood that it is essential to isolate the system well from its environment in order to suppress decoherence [1]. However, there are several results that suggest that this is not sufficient, and that the precision of the measurements that one is able to perform on the system also plays an important role.

The first example we are aware of is Mermin's work in 1980 [2]. He showed that in order to obtain a Bell inequality violation for singlet states of two large spins s, the directions of the spin measurements had to be chosen with an angular resolution that increased with the size of the spins as $1/s$. Note that here and in the following we speak of 'increasing' resolution or precision when the acceptable error or uncertainty decreases. The requirement of choosing the spin direction precisely is an example for necessary *control precision*, a concept that will be important for what follows.

Later Peres [3] showed that for the same singlet state of two spins the precision with which the measurement outcomes are known is also important. He showed that if this *outcome precision* is worse than $O(\frac{1}{\sqrt{s}})$ in relative terms (i.e. dividing the measurement error by the absolute value of the spin), then a classical model can reproduce the quantum predictions for the correlation functions. Related results for individual large spins were obtained in Ref. [4]. Ref. [5] which studied multi-photon singlet states equivalent to Mermin's and Peres' spin singlets and showed that $O(\frac{1}{\sqrt{N}})$ relative outcome precision is sufficient to demonstrate entanglement. Here the photon number N quantifies the size of the system in the same way as s does for the spin examples.

More recently it was shown [5] for closely related multi-photon singlet states that their entanglement can be demonstrated if photon counting measurements have a resolution better than $\sqrt{N}$, where N is the total number of photons. Most recently, Ref. [6] showed that for multi-photon states based on amplifying one half of an initial two-photon entangled state,

micro-macro entanglement can be demonstrated only if photons can be counted with single-photon level precision. In Ref. [6] it was conjectured that showing macroscopic quantum effects generally requires highly precise measurements, even in the absence of decoherence.

The multi-photon states considered in Refs. [5, 6] can be created by χ_2 non-linearities with a classical pump field, or more formally by generalized squeezing transformations. The associated Heisenberg equations of motion correspond to a linear mixing of creation and annihilation operators. This may lead one to question the generality of a conjecture based on such a relatively special class of states. The question is made more urgent by the results of Ref. [9], which showed that using a Kerr (χ_3) non-linearity, for which the dynamics of field operators is also non-linear, it is possible to implement states and measurements that allow one to violate a Bell inequality using very coarse-grained homodyne detection. Does this mean that higher-order non-linearities make it fundamentally easier to observe macroscopic quantum effects? Similar questions concerning the usefulness of non-linearities have been raised in quantum metrology [7].

Here we show that in the present context there is a significant price to pay. We are not referring to the practical difficulty of implementing strong Kerr non-linearities. While this is still an open challenge, there are several promising recent proposals [8, 9]. In the spirit of the above discussion, we are also not concerned with the high sensitivity of the relevant multi-photon states to photon loss. Loss is due to the coupling of the system to its environment, whereas here we are interested in fundamental limits to the observability of macroscopic quantum effects even when the system is completely isolated.

We found that there is a difficulty that is - in a sense - complementary to the precision requirements on photon number measurements discussed in Refs. [5, 6]. Namely, the *phase* of unitary operations involving the Kerr non-linearity has to be extremely well defined. This can be shown by analyzing the evolution of the cat state in Kerr medium, which has just been experimentally acheived recently [16]. By caculating the characteristic phase (or correspond

to characteristic time if we consider the nonlinear coefficient as perfect constant) when the cat state collapse, we found that the required phase precision scales like $N^{-\frac{1}{2}}$, where N is the mean number of photons.

3.3 Coarse-grained measurement scheme

We will begin by describing a conceptually simple scheme based on Kerr non-linearities that in principle allows the coarse-grained detection of macroscopic entanglement, see Fig. 1. Our scheme can be seen as a simplified version of the proposal of Ref. [9]. It is different from that proposal both concerning the state that is used and the final measurements that are performed, but the phase precision requirements shown here apply to Ref. [9] as well. We use the interaction Hamiltonian for a Kerr non-linearity,

$$H_{KNL} = K(a^\dagger a)^2, \tag{3.1}$$

where K is the coupling constant and a is the annihilation operator for the relevant mode. We first use the interaction for a non-linear phase $Kt = \frac{\pi}{2}$ to create a superposition of coherent states from an initial coherent state $|\sqrt{2}\alpha\rangle$ following Ref. [11],

$$|\psi_0\rangle = e^{-i\frac{\pi}{2}n^2}|\sqrt{2}\alpha\rangle = \frac{e^{-i\pi/4}}{\sqrt{2}}(|\sqrt{2}\alpha\rangle + i|-\sqrt{2}\alpha\rangle), \tag{3.2}$$

where we are interested in the regime $\alpha \gg 1$ (we will take α to be real for simplicity). Sending this state onto a 50/50 beam splitter creates an entangled superposition of coherent states [19],

$$\frac{e^{-i\pi/4}}{\sqrt{2}}(|i\alpha\rangle_A|\alpha\rangle_B + i|-i\alpha\rangle_A|-\alpha\rangle)_B, \tag{3.3}$$

where we have introduced two parties A and B corresponding to the two modes after the beam splitter. For $\alpha \gg 1$ this can be seen as a maximally entangled state of "coherent-state qubits" with basis states $|\alpha\rangle$ and $|-\alpha\rangle$ that are almost orthogonal. In order to measure an entanglement witness such as a Bell inequality on such a state we require two more

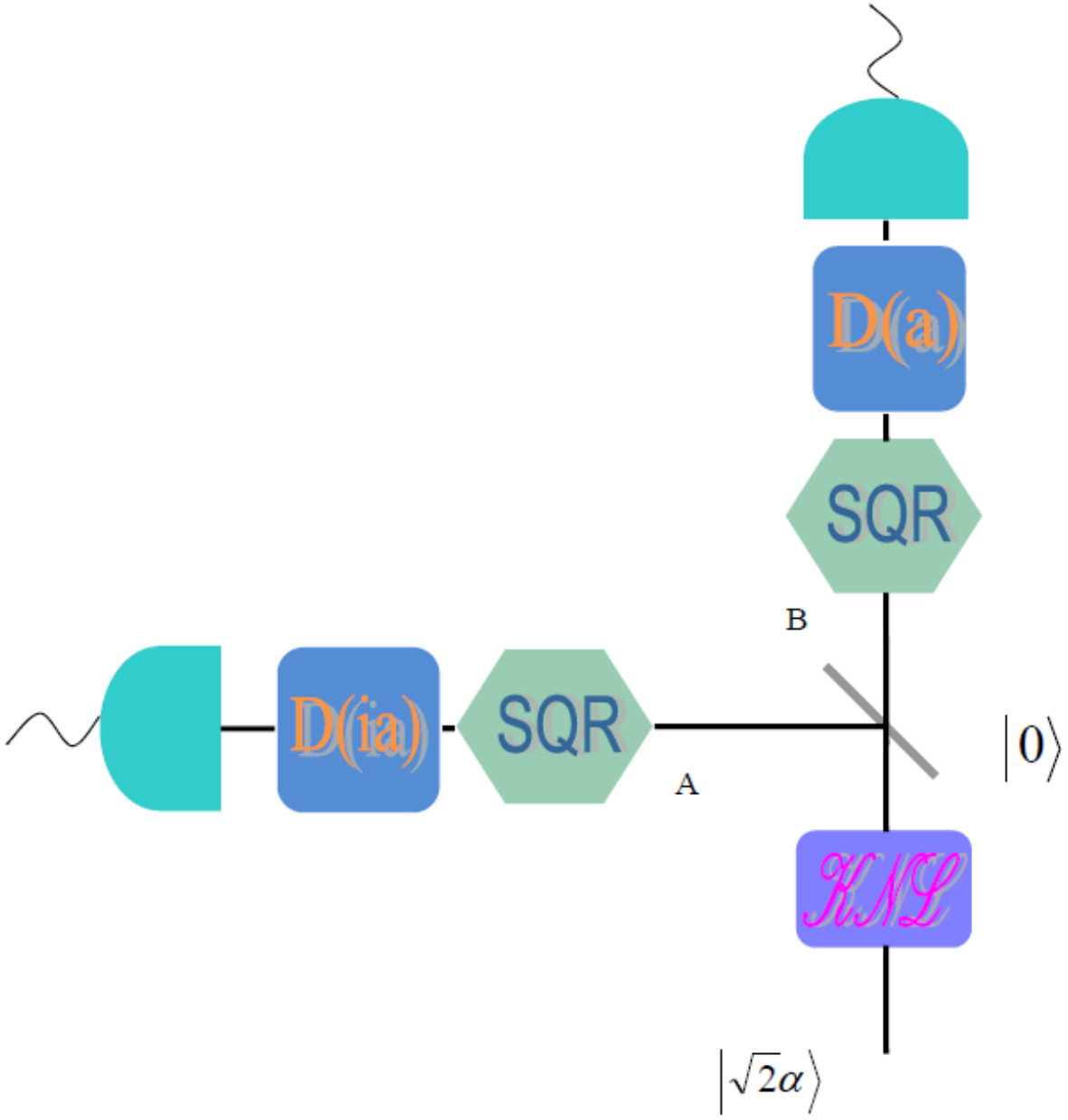

Figure 3.1: **Scheme to observe macroscopic entanglement with very coarse-grained measurements.** The coherent state $|\sqrt{2}\alpha\rangle$ (with $\alpha \gg 1$) is transformed into a macroscopic superposition of coherent states Eq. (3.2) using a Kerr non-linear operation (KNL). The superposition is transformed into a maximally entangled state of coherent state qubits Eq. (3.3) using a beam splitter. General single-qubit rotations (SQR) can be implemented using the Kerr nonlinearity following Ref. [16]. Detection in the coherent state qubit basis is done via the displacement of $D(\alpha)$, followed by detectors that only need to distinguish the bright state $|\sqrt{2}\alpha\rangle$ from the vacuum, as shown in Fig. 3.5. This setup would in principle allow the observation of Bell inequality violations (for example), thus demonstrating macroscopic entanglement.

ingredients, namely single-qubit rotations and measurements in the qubit basis. In Ref. [16] it was shown that arbitrary single-qubit rotations can be implemented by combining the same Kerr non-linear operation that was used to create the initial coherent state superposition in Eq. (3.2) with small displacements in phase space, where the latter can be implemented using a strongly asymmetric beam splitter; in particular see Eqs. (9), (10) and (5) of Ref. [16].

The final missing ingredient is then the measurement in the qubit basis, i.e. a measurement that allows one to distinguish the states $|\alpha\rangle$ and $|-\alpha\rangle$. Such a measurement can be performed by implementing a displacement operator $D(\alpha)$. That is, for the input state $|\alpha\rangle$ the output will be a strong coherent beam, whereas for the input state $|-\alpha\rangle$, the output mode will be dark, as shown in Fig.5. The two states can then easily be distinguished by highly coarse-grained photon counting because all that is required is to distinguish a very bright state from the vacuum. The use of a strong Kerr non-linearity thus makes it possible to avoid the high-resolution requirement discussed in Ref. [6], at least as far as photon counting is concerned. This confirms the result of Ref. [9] that it is *in principle* possible to observe a violation of Bell's inequality with very coarse-grained measurements.

3.4 Extremely high requirement of nonlinear phase control

We now show that there is a significant difficulty with this approach. The Kerr operation of Eq. (3.2), which also intervenes in the single-qubit rotations following Ref. [16], requires very high phase resolution. If the phase is not precisely controlled, the cat state will collapse very quickly for large mean photon numbers, which makes the experimental scheme unsuccessful.

3.4.1 Rotation and deformation effects of cat state evolution in Kerr medium

The dispersion of the cat state as the result of the imprecision of the phase control, can be shown by the Husimi Q function $Q(\beta)$, which is commonly used to visualize the evolution of

the coherent state in Kerr medium. Experimental observation of the Q function evolution of coherent state in Kerr medium has being achieved recently [16]. $Q(\beta)$ is defined in a space spanned by the expectation value of the dimension-less field quadrature $Re(\beta)$ and $Im(\beta)$ as $Q(\beta) = \frac{|\langle\beta|\psi_\phi\rangle|^2}{\pi}$. And

$$|\psi_\phi\rangle = e^{-i(\frac{\pi}{2}+\phi)n^2}|\sqrt{2}\alpha\rangle \tag{3.4}$$

$$= e^{-\frac{N}{2}}\sum_n e^{-i(\frac{\pi}{2}+\phi)n^2}\frac{N^{n/2}}{\sqrt{n!}}|n\rangle \tag{3.5}$$

Here ϕ is the phase error due to the imprecision of the phase control.

In Fig. 2 we plot the Q function evolution of the cat states in Kerr medium with mean photon number N=16, 64, 256.

From the picture we can see that as the error of the non-linear phase increases, the cat state rotates in the phase space. At the same time it is getting deformed. Eventually, the two components merge together and is evenly distributed in a circle in the phase space, thus the cat state "collapses. This cat state evolution is quite similar to the coherent state evolution discussed in Ref.[17].

From Fig. 2 we can see that both the rotation and deformation occur faster with larger mean photon number. These could be understood analytically as follows.

The rotation effect is similar to the evolution under a rotation Hamiltonian $H_{ROT} = 2KNa^\dagger a$. Here N is the mean photon number. Fig. 3.3 compares the cat state evolution under H_{ROT} and the Kerr Hamiltonian H_{KNL}. This could also be confirmed by the following calculation:

$$e^{-iH_{KNL}t}|cat\rangle = e^{-\frac{N}{2}}\sum_n e^{-i\phi n^2}e^{-i\frac{\pi}{2}n^2}\frac{N^{n/2}}{\sqrt{n!}}|n\rangle = e^{-\frac{N}{2}}e^{-i\phi N^2}\sum_l e^{-i\phi(2Nl+l^2)}\frac{e^{-i\frac{\pi}{2}(N+l)^2}N^{(N+l)/2}}{\sqrt{(N+l)!}}|N+l\rangle \tag{3.6}$$

$$e^{-iH_{ROT}t}|cat\rangle = e^{-\frac{N}{2}}\sum_n e^{-i\phi 2Nn}e^{-i\frac{\pi}{2}n^2}\frac{N^{n/2}}{\sqrt{n!}}|n\rangle = e^{-\frac{N}{2}}e^{-i2\phi N^2}\sum_l e^{-i\phi 2Nl}\frac{e^{-i\frac{\pi}{2}(N+l)^2}N^{(N+l)/2}}{\sqrt{(N+l)!}}|N+l\rangle \tag{3.7}$$

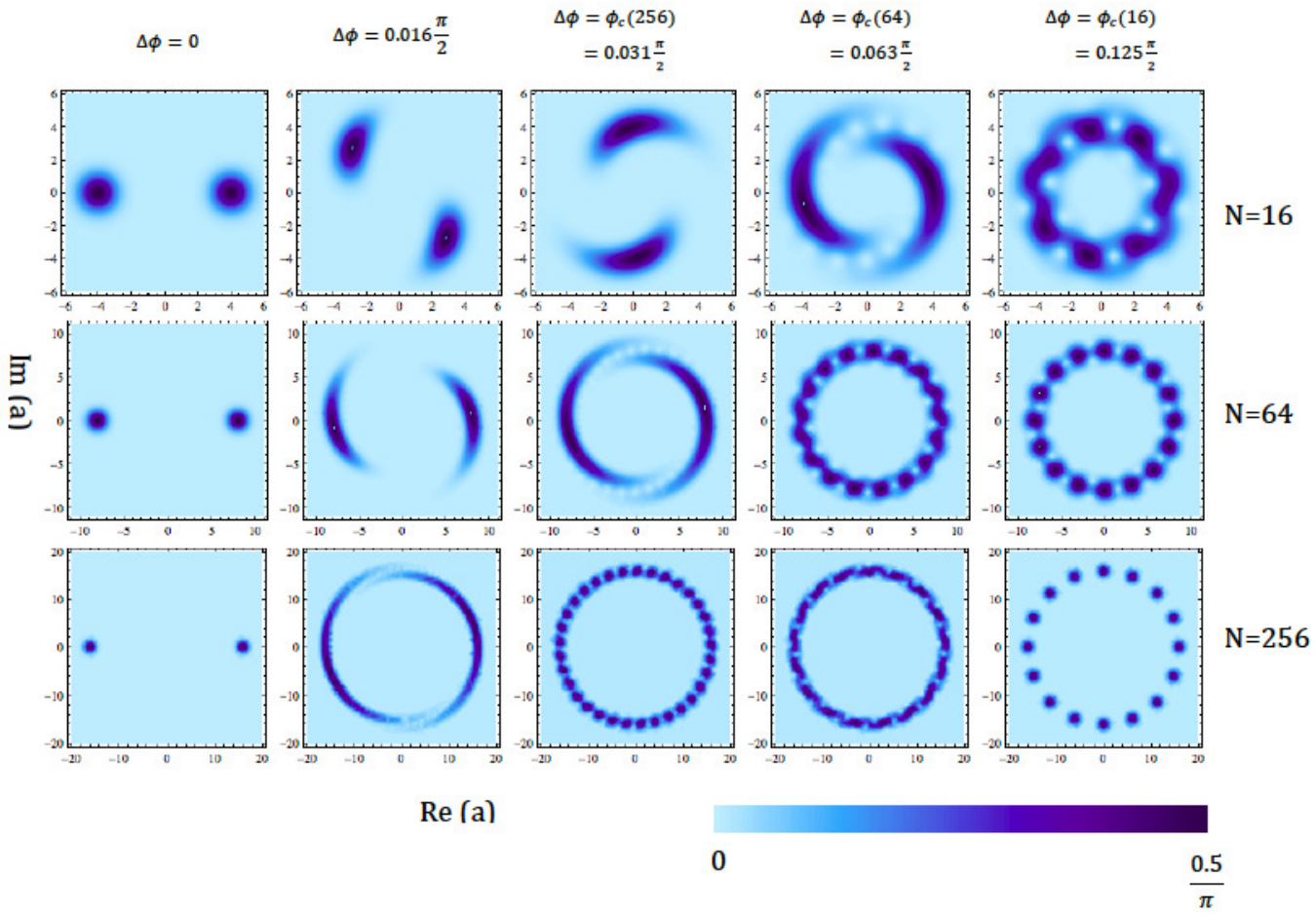

Figure 3.2: **Q function evolution of the cat states with mean photon number N=16, 64, 256 in the Kerr medium.**
The Q function of ideal cat state is two Gaussian packets. As the phase error ϕ increases, the two components of the cat state get deformed. When ϕ reaches the characteristic phase $\phi_c(N) = \frac{\pi}{4\sqrt{N}}$ Eq. (3.4.2), the two components completely merge with each and the cat state "collapses. From the picture we can see that the cat state collapses more and more quickly with increasing mean photon number N. When $\phi = 0.031\frac{\pi}{2}$, the characteristic phase of N=256 cat state, the two components of N=16 cat state is still distinguishable, while the two components of N=64 cat state already begins to merge, and for N=256 cat state, the two components are evenly distributed in the whole phase, which indicates the cat state collapse.

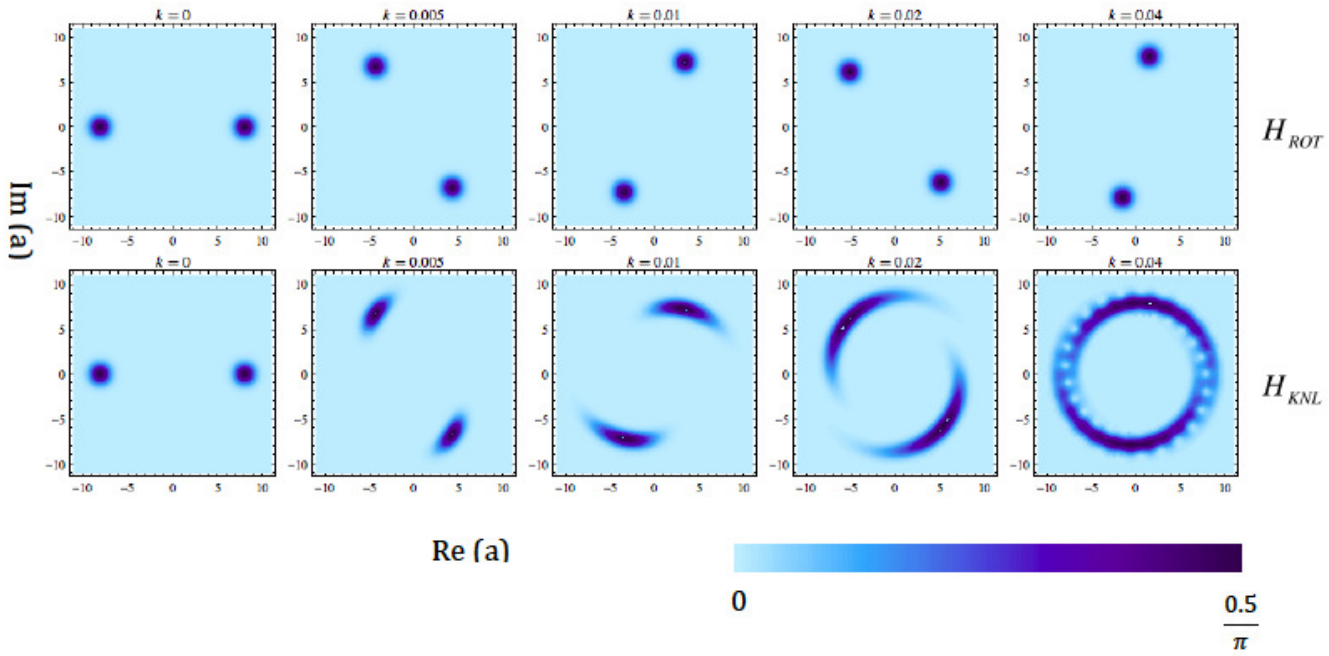

Figure 3.3: **Q function evolution of the cat states with mean photon number N=64 with H_{ROT} and the Kerr Hamiltonian H_{KNL}.** It could be seen that the rotation effect of the Kerr evolution has angular speed that is the same with the the speed of the rotation proportional to the mean photon number N.

Here we changed the summation index $n = N + l$. By the above comparison, it is obvious that $e^{-i\phi 2Nl}$ correspond to the rotation effect, and $e^{-i\phi l^2}$corresponds to the deformation effect. According to the photon number distribution of the coherent state, the majority of the number states range from $l = -\sqrt{N}$ to $\sqrt{N}$, thus the rotation would scale like $N^{-\frac{3}{2}}$, and the deformation scales like N^{-1}. Both effect increase as mean photon number increases.

Here we define the fidelity $F(\phi)$ as the overlap between an ideal cat state and the real state with phase error $F = |\langle\psi_0|\psi_\phi\rangle|^2$, and plot it in Fig. 3.5 for N=16, 64, 256 respectively. From the picture we can see that the fidelity decreases dramatically with phase error. This could be understood intuitively as that the real states rotate quickly away from the ideal state in phase space, resulting the overlap approaching zero. The scaling of the fidelity can be shown to be the same with that of the rotation effect. One has

$$\langle\psi_\phi|\psi_0\rangle = e^{-N}\sum_{n=0}^{\infty}\frac{N^n}{n!}e^{i(\phi-\frac{\pi}{2})n^2}. \tag{3.8}$$

Using the Stirling expansion for $\ln n!$, defining $x = n - N$ and $\tilde{\phi} = \phi - \frac{\pi}{2}$, approximating the sum over x by an integral, and keeping only the terms that are dominant in the limit of large N, one finds that this is proportional to

$$\int_{-\infty}^{\infty} e^{-\frac{x^2}{2N}}e^{i2N\tilde{\phi}x}dx, \tag{3.9}$$

where the proportionality factor can be inferred from the fact that the overlap is equal to one for $\tilde{\phi} = 0$. Performing the integral gives a Gaussian distribution for $\tilde{\phi}$ whose width scales like $N^{-\frac{3}{2}}$, in good correspondence with the results shown in Fig. 1 [14].

We can also define another fidelity F_d which characterize the deformation effect by canceling the rotation effect.

$$F_d(\phi) = |\langle\psi_0|e^{-i\phi}|\psi_\phi\rangle|^2 = |e^{-N}\sum_{n=0}^{\infty}\frac{(Ne^{iN\phi})^n}{n!}e^{-i\phi n^2}|^2 \tag{3.10}$$

In Fig. 3.5 we plot $F_d(\phi)$ for N=16, 64, 256 states so as to illustrate the deformation effect. It is obvious that the overlap decrease more quickly with larger N.

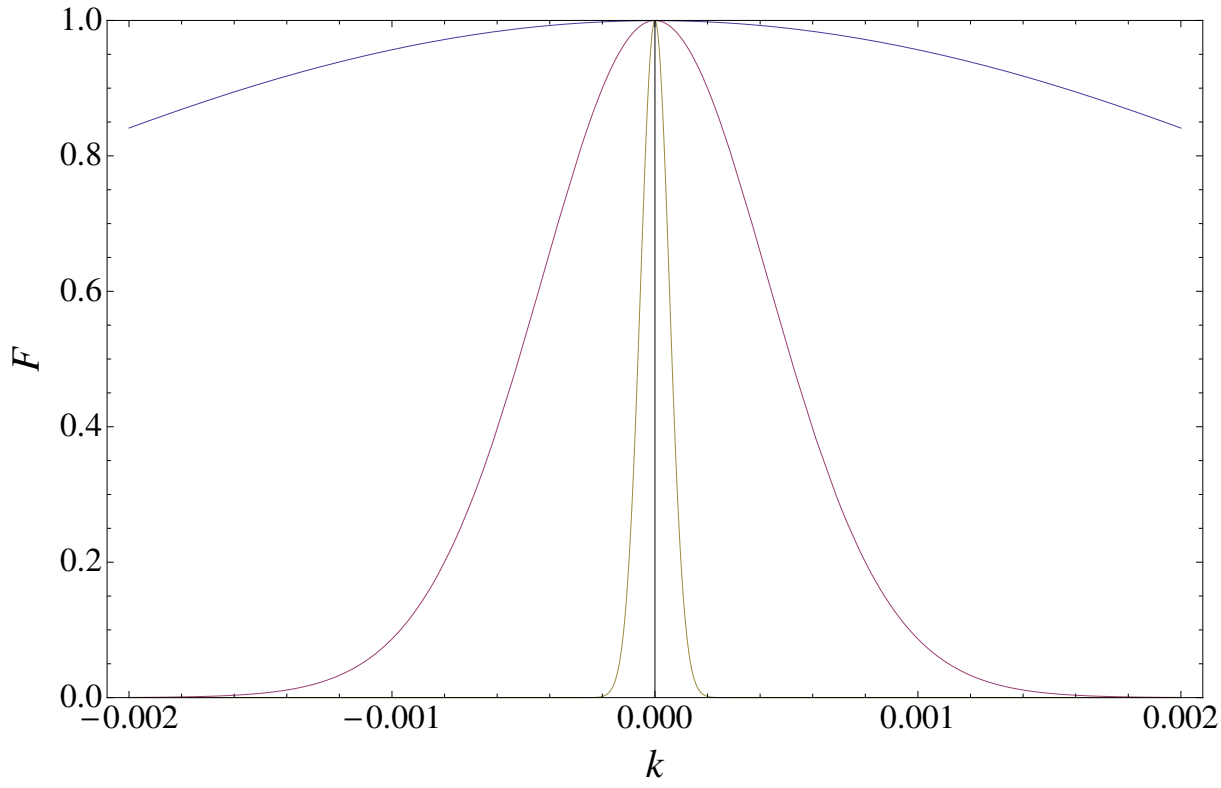

Figure 3.4: **Fidelity $F(\phi)$ of the state $|\psi_\phi\rangle$ of Eq. (3.5) relative to the ideal state $|\psi_0\rangle$ of Eq. (3.2) for different values of N.** $F(\phi)$ is a function of the non-linear phase errorϕ. The curves correspond to mean photon numbers $N = 2\alpha^2$ equal to 16, 64 and 256 from top to bottom. The fidelity decays faster and faster as the mean number of photons increases.

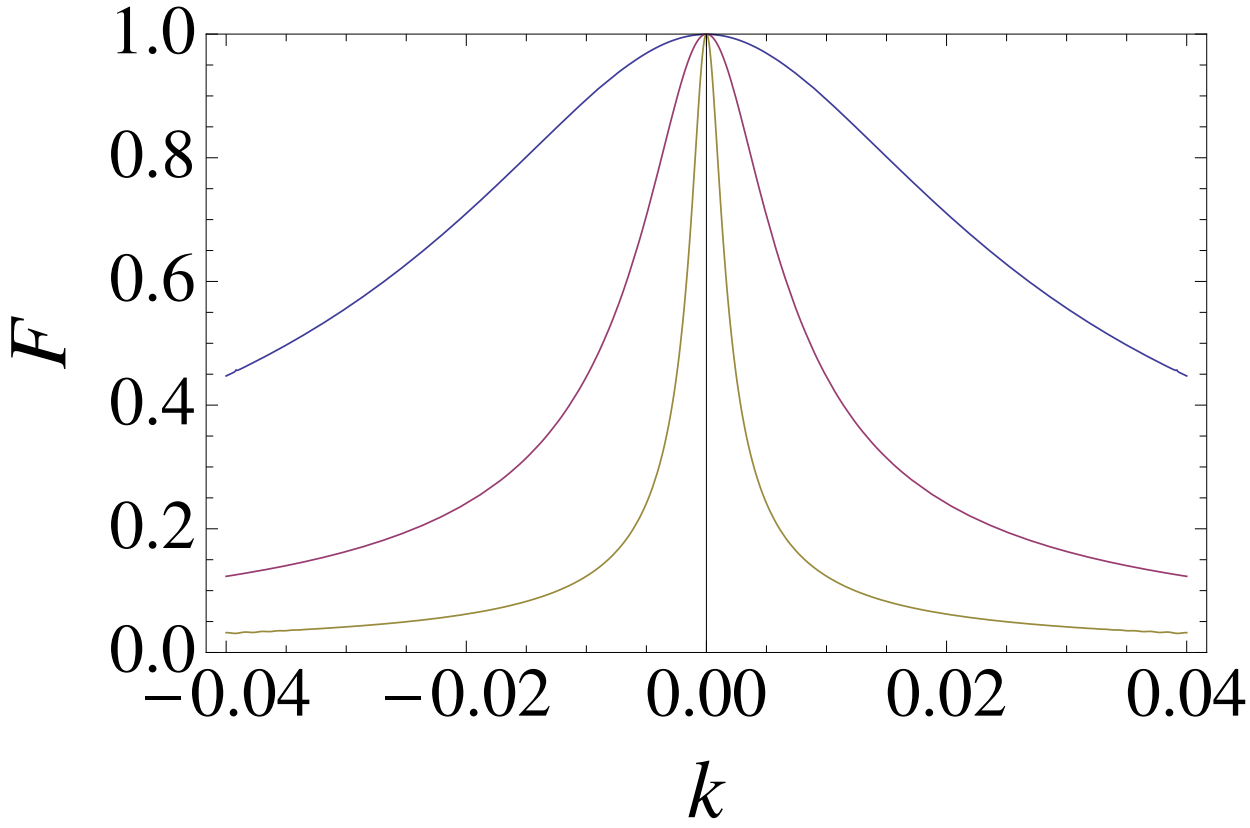

Figure 3.5: **Overlap $F_d(\phi)$ illustrating the deformation effect in the Kerr medium due to the phase error.** $F_d(\phi)$ is a function of ϕ which measures the non-linear phase error. The curves correspond to mean photon numbers $N = 2\alpha^2$ equal to 16, 64 and 256 from top to bottom. The fidelity decays faster and faster as the mean number of photons increases.

3.4.2 Characteristic phase when the cat state "collapse due to phase error

In real experiments, although very difficult, there might still be a possibility to cancel the rotation effect by rotating the initial state back. However, the effect of deformation which eventually make the cat state collapse is hard to compensate. And it is this effect, which increases drastically with increasing photon numbers, that makes the above scheme impossible. This is because that the the coarse grained measurement relies on displacing the cat state in the phase space, making the difference of the mean photon number of the two components very large so that a very coarse grained photon number measurement is able to differentiate them. This scheme still holds when each component of the cat state is a little deformed, since the difference of mean photon number of the two components of the cat state is still very large after displacement. However, if the two components completely merge with each other and get evenly distributed in the phase space, the mean photon number difference would be zero, thus the coarse grained measurement ceases to work, as illustrated in Fig. 3.6.

The characteristic phase ϕ_c when the two components are completely merged together is similar to the corresponding collapse time of the coherent state in Ref. [15]. The latter can be obtained by computing the expectation value $\langle a\rangle$ of the field operator over the coherent state under Kerr nonlinear evolution $|\psi_\phi\rangle = e^{-i\phi H_{KNL}}|\sqrt{2}\alpha\rangle$

$$\langle a\rangle = \langle\psi_\phi|a|\psi_\phi\rangle = \alpha e^{-N}\sum_n \frac{N^{n-1}}{(n-1)!}e^{-i\phi_c(2n+1)} \tag{3.11}$$

$$= -\alpha e^{-N}e^{i\phi_c}\sum_n \frac{N^{n-1}}{(n-1)!}e^{-i2n\phi_c} \tag{3.12}$$

As we know, a coherent state can be expressed as a superposition of number states. However, the phase error of the nonlinear interaction will result in the n-dependent phase distribution of each number state, which is $2n\phi_c$. For an ideal coherent state the width of the photon number distribution is $2\sqrt{N}$. By replacing n with $2\sqrt{N}$, we obtain the difference of the phase of the two ends of the photon number distribution $4\sqrt{N}\phi_c$, which we name

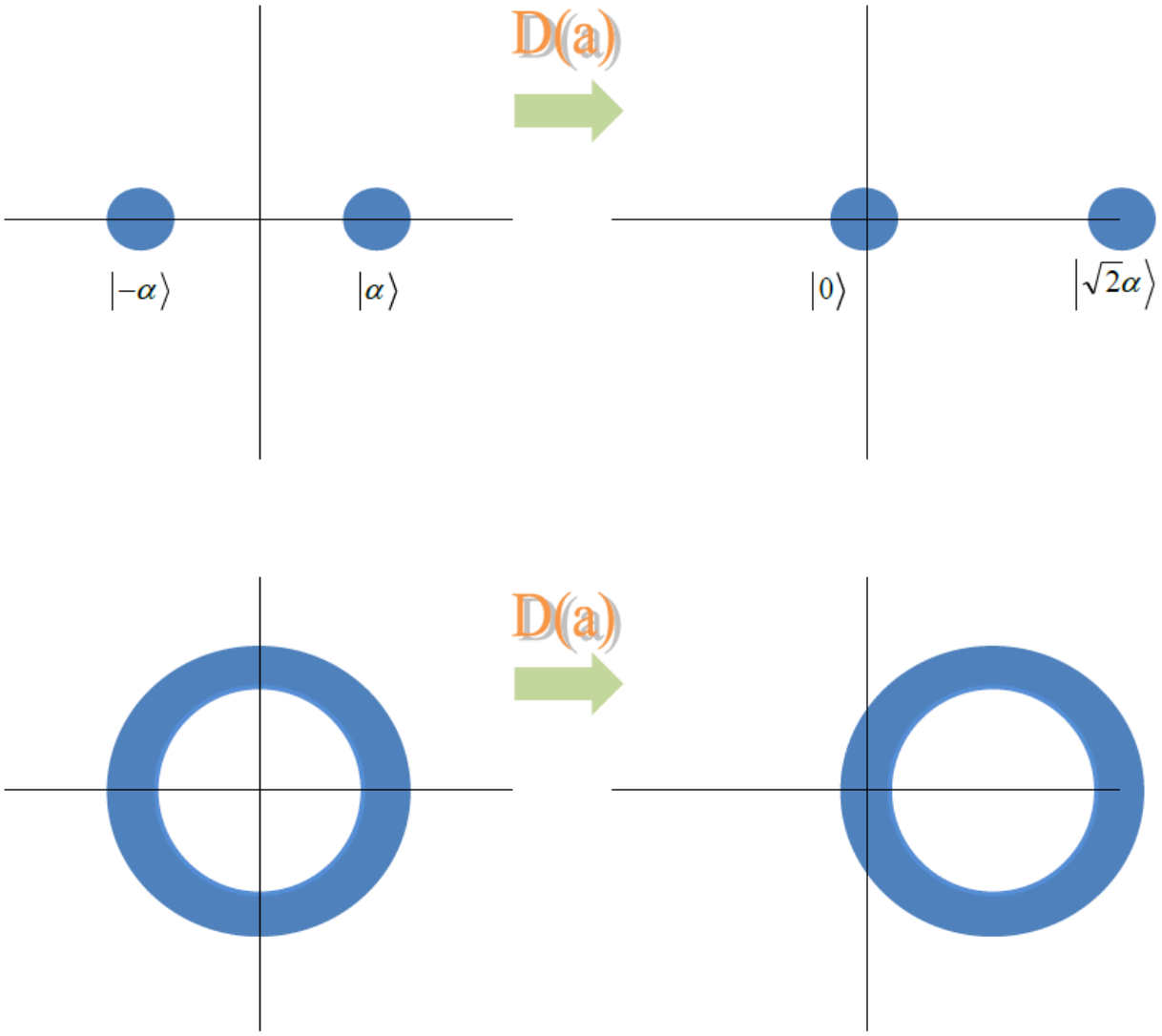

Figure 3.6: **The complete deformation would make the scheme unsuccessful.** The deformation due to the phase error, which increases drastically with increasing photon numbers, makes the above scheme impossible. This is because the coarse grained measurement relies on displacing the cat state in the phase space, making the difference of the mean photon number of the two components very large so that a very coarse grained photon number measurement is able to differentiate them, as shown in the upper pictures. This scheme still hold when each component of the cat state is a little deformed, since the difference of mean photon number is still very large after displacement. However, if the two components completely merge with each other and get evenly distributed in the phase space, the mean photon number difference would become zero, thus the coarse grained measurement ceases to work

as dispersion. When this phase dispersion becomes π, the state is generally considered as collapsed, which yields the characteristic phase ϕ_c

$$\phi_c = \frac{\pi}{4\sqrt{N}} \tag{3.13}$$

For N=16, 64, 256, $\phi_c = 0.125, 0.063, 0.031$ respectively.

This also indicates that the cat state collapses more and more quickly as the mean photon number increases. As shown in Fig. 3.6, at $\phi_c/2$ the two components of each cat state already spread by more the 180° degree and begin to smear. At ϕ_c, each component is evenly distributed in the phase space and we can no longer distinguish between the two components. This clearly shows that the cat state has totally collapsed, making the coarse grained measurement cease to work. The need for extreme phase resolution (for $\alpha \gg 1$) applies both to our scheme and to the scheme of Ref. [9], which uses the Kerr nonlinearities in a similar way. It also applies to the original proposal of Ref. [11] for generating macroscopic superpositions of coherent states.

3.5 conclusion

In conclusion, the evolution of the cat state due to the imprecision of the phase control, which is increasingly significant with increasing mean photon number, would make it extremely difficult to observe macroscopic entanglement, even with coarse-grained measurement. These results show that while it is in principle possible to observe macroscopic quantum effects with very coarse-grained photon *number* measurements in this system, one has to pay the price of requiring increasingly precise (as the size of the system increases) *phase* control for the operations involving the Kerr non-linearity. It should be noted that although it is possible to make the strength of available Kerr nonlinearities extremely small, so as to have long evolution time, which is relatively easier to control, this would help to increase the precision of the non-linear phase control. This is because for very small nonlinearities it would be very

difficult to distinguish between 0.00021 and 0.00022, for example. In this case, although the evolution time may be precisely controlled, the total phase imprecision is still considerable.

The result supports the idea that there may be a general principle that makes it hard to observe macroscopic quantum phenomena, even in the absence of environmentally induced decoherence. The precise form of this principle remains to be discovered. Comparing the present results to those of Ref. [6] one is tempted to conjecture the existence of a photon number-phase trade-off (similar to an uncertainty relation), which would imply that observing quantum effects in macroscopic systems requires either very precise photon number measurements or very precise phase control. However, it should be noted that the phase considered here is that of a non-linear operation, which is a different concept from the phase observable that is complementary to photon number in several respects, including the fact that it is a control parameter and not an observable. Note that Mermin's result in Ref. [2] concerns a control parameter, while the results of Refs. [3, 5, 6] concerns the precision of measurements. It may be possible to gain more insight into these questions by studying further examples. In particular, it would be interesting to find cases where there are trade-offs between the requirements for number and phase precision, and also between control precision and measurement precision.

Bibliography

[1] W.H. Zurek, Rev. Mod. Phys. **75**, 715 (2003).

[2] N.D. Mermin, Phys. Rev. D **22**, 356 (1980).

[3] A. Peres, *Quantum Theory: Concepts and Methods* (Klouwer, 2002); see also J. Kofler and C. Brukner, Phys. Rev. Lett. **99**, 180403 (2007) for related results on individual large spins.

[4] C. Simon and D. Bouwmeester, Phys. Rev. Lett. **91**, 053601 (2003).

[5] S. Raeisi, P. Sekatski, and C. Simon, Phys. Rev. Lett. **107**, 250401 (2011).

[6] H. Jeong, M. Paternostro, and T.C. Ralph, Phys. Rev. Lett. **102**, 060403 (2009).

[7] M. Napolitano *et al.*, Nature **471**, 486 (2011).

[8] I. Friedler, D. Petrosyan, M. Fleischhauer, and G. Kurizki, Phys. Rev. A **72**, 043803 (2005).

[9] A. Rispe, B. He, and C. Simon, Phys. Rev. Lett. **107**, 043601 (2011).

[10] B. Yurke and D. Stoler, Phys. Rev. Lett. **57**, 13 (1986).

[11] B.C. Sanders, Phys. Rev. A **45**, 6811 (1992).

[12] H. Jeong and M.S. Kim, Phys. Rev. A **65**, 042305 (2002).

[13] C. Branciard, N. Gisin, and V. Scarani (private communication, 2006).

[14] There is some similarity between this result and those of W.H. Zurek, Nature **412**, 712 (2001), who studied the sensitivity of "cat states" such as that of Eq. (2) to displacements. In contrast, here we discussed their sensitivity to changes in the non-linear operation that is used to create them.

[15] S. Haroche, J. M.Raimond, Exploring the Quantum. Atoms, Cavities, And Photons, Section 7.2 (Oxford University Press, USA, 2006).

[16] Gerhard Kirchmair, Brian Vlastakis, Zaki Leghtas, Simon E. Nigg, Hanhee Paik, Eran Ginossar, Mazyar Mirrahimi, Luigi Frunzio, S. M. Girvin, R. J. Schoelkopf, arixv 1211.2228.

[17] M. Kitagawa and Y. Yamamoto, Phys. Rev. A 34, 3974?3988 (1986)

Chapter 4

Precision requirements for observing macroscopic quantum effects

4.1 Preface

It has recently been conjectured that detecting quantum effects such as superposition or entanglement for macroscopic systems always requires high measurement precision. Analyzing an apparent counter-example involving macroscopic coherent states and Kerr non-linearities, we find that while measurements with coarse outcomes can be sufficient, the phase control precision of the necessary non-linear operations has to increase with the size of the system. This suggests a refined conjecture that either the *outcome precision* or the *control precision* of the measurements has to increase with system size.

In this chapter we continue to discuss the topic of precision requirements to observe macroscopic quantum effects, in a more general form. This chapter is based on the paper "*Precision requirements for observing macroscopic quantum effects*" Phys. Rev. A 88, 062114 (2013). My contribution is that I did the calculations, drew the graphs, and helped write the paper and correspond with the referees.

4.2 Introduction

What does it take to observe quantum effects such as superposition and entanglement for macroscopic systems? It is essential to isolate the system well from its environment in order to suppress decoherence [1]. However, there are several results that suggest that this is not sufficient, and that the precision of the measurements that one is able to perform on the system also plays an important role. Mermin [2] showed in 1980 that in order to obtain

a Bell inequality violation for singlet states of two large spins s, the directions of the spin measurements had to be chosen with an angular resolution that increased with the size of the spins as $1/s$. Note that here and in the following we speak of 'increasing' resolution or precision when the acceptable error or uncertainty decreases. The requirement of choosing the direction precisely is an example for necessary measurement *control precision*, i.e. the precision with which relevant physical parameters have to be controlled in order to implement the desired measurement procedure.

Later Peres [3] showed that for the same singlet state of two spins the precision with which the measurement outcomes are known is also important. He showed that if this measurement *outcome precision* is worse than $O(\frac{1}{\sqrt{s}})$ in relative terms, then a classical model can reproduce the quantum predictions for the correlation functions. Related results for individual large spins were obtained in Ref. [4]. Ref. [5] studied multi-photon singlet states equivalent to Mermin's and Peres' spin singlets and showed that $O(\frac{1}{\sqrt{N}})$ relative outcome precision (where N is the photon number) is sufficient to demonstrate entanglement. Most recently Ref. [6] studied so-called micro-macro entangled states of light that are obtained by greatly amplifying one half of an initial entangled photon pair. These authors found that a relative outcome precision of order $\frac{1}{N}$ was necessary to see quantum effects in this example. Similar results on the effect of coarse-graining on macroscopic entanglement were found in Refs. [7, 8].

Ref. [6] also put forward the conjecture that demonstrating quantum effects in macroscopic systems always requires high measurement precision. In contrast, Ref. [9] proposed a state and measurement procedure based on the use of Kerr non-linearities where a Bell inequality violation could apparently be observed with very coarse measurements. As a first step towards addressing this apparent contradiction, Ref. [6] pointed out that the non-linear operations used in the proposal of Ref. [9] involve large (π) phase shifts between neighboring Fock states and suggested that this could be seen as high resolution in a more general sense.

Later the previous chapter showed that in order to prepare entangled states of the type used in Ref. [9] the phase of the non-linear operations has to be controlled with a precision that increases with system size. Chapter 3 is linked to the present work in that it already highlighted the importance of phase precision. However, it focused on state preparation. Here we explicitly address the question of measurement precision posed in Ref. [6]. We show that even if one assumes that the states under consideration are ideal, measurement precision - in particular control precision - has to increase with system size in order to be able to demonstrate quantum effects.

This chapter is organized as follows. Section II shows how the requirement of high outcome precision arises in the context of quadrature measurements on macroscopic superposition states. Section III shows that this requirement can be avoided if Kerr or higher nonlinearities are available, but also that a complementary requirement of high control precision arises in this case. Section IV shows that the same requirements apply to macroscopic entanglement. In Sec. V we present and discuss our refined conjecture.

4.3 Macroscopic superpositions: requirement for high outcome precision

We study superpositions and entanglement involving coherent states with opposite phase, $|\alpha\rangle$ and $|-\alpha\rangle$, where we will take α to be real for simplicity. We will pay particular attention to the macroscopic limit $\alpha \gg 1$. We study this example not only because these states lie at the heart of the proposal of Ref. [9], but also because they are a well-known "archetype" for macroscopic quantum superpositions [11, 12, 13]. Let us note right away that the proposal of Ref. [9] is more complex than the simple cases considered here. However, our conclusions concerning control precision apply to that work as well. We focus on simple states and measurement schemes for clarity.

We begin by considering the superposition state

$|\alpha_+\rangle = \frac{1}{\sqrt{2}}(|\alpha\rangle + i|-\alpha\rangle)$,

focusing on the regime where α is large enough such that the overlap $\langle\alpha|-\alpha\rangle = e^{-2\alpha^2}$ is negligible. The phase factor i is chosen for convenience. This state can be created, for example [11, 13], from an initial coherent state with the help of a Kerr nonlinearity,

$$e^{-i\frac{\pi}{2}\hat{N}^2}|\alpha\rangle = e^{-i\frac{\pi}{4}}|\alpha_+\rangle, \tag{4.1}$$

where $\hat{N} = a^\dagger a$, and a is the bosonic annihilation operator for which the coherent state is an eigenstate, $a|\alpha\rangle = \alpha|\alpha\rangle$. It was shown in Ref. [10] that the phase of the unitary operation in Eq. (4.1) has to be precisely equal to $\frac{\pi}{2}$ in order to generate this state with high fidelity, with a precision that increases with α. However, as mentioned in the introduction, this is not our concern here. We will assume that the ideal state is given to us and focus on the question of how to prove that we have a quantum superposition state, as opposed to a "classical" mixture of the same two coherent states,

$$\rho = \frac{1}{2}(|\alpha\rangle\langle\alpha| + |-\alpha\rangle\langle-\alpha|). \tag{4.2}$$

Let us first consider measurements of the quadrature $\hat{x} = \frac{1}{2}(a + a^\dagger)$. For the state of Eq. (**??**), this will give a symmetric bimodal distribution of results corresponding to the two components of the superposition,

$$P(x) = |\langle x|\alpha_+\rangle|^2 = \frac{e^{-(x+\alpha)^2} + e^{-(x-\alpha)^2}}{2\sqrt{\pi}}, \tag{4.3}$$

where $\hat{x}|x\rangle = x|x\rangle$. Note that for $\alpha \gg 1$ one can distinguish the two components using very coarse measurements of $\hat{x}$; this point will be significant below. However, this does not prove that one is dealing with a macroscopic superposition state, since the mixed state of Eq. (4.2) will produce the exact same distribution of outcomes. In general, one has to measure at least two *non-commuting* observables in order to prove the quantum character of any system. One obvious choice for an observable that does not commute with $\hat{x}$ is the complementary quadrature, $\hat{p} = \frac{-i}{2}(a - a^\dagger)$. The probability distribution of the associated outcomes p is

$$P_{|\alpha+\rangle}(p) = |\langle p|\alpha_+\rangle|^2 = \frac{e^{-p^2}(1 - \sin(2\alpha p))}{\sqrt{\pi}} \tag{4.4}$$

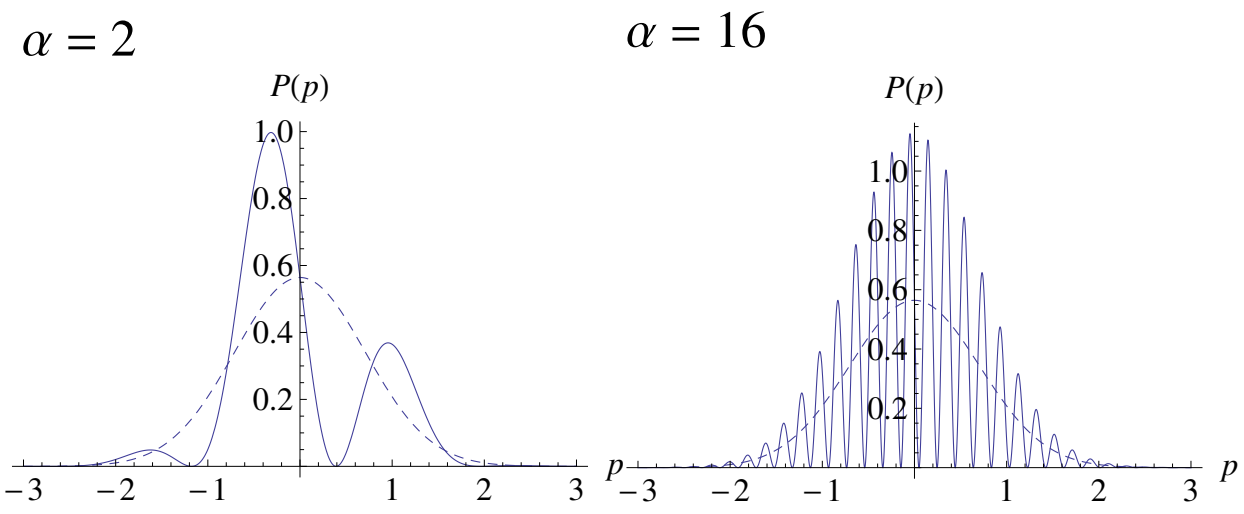

Figure 4.1: Probability of outcomes for measurements of the $\hat{p}$ quadrature for the superposition state $|\alpha_+\rangle$ and the mixed state of Eq. (4.2) for $\alpha = 2$ (left) and $\alpha = 16$ (right). The oscillatory structure that distinguishes the two distributions becomes harder to resolve as α increases, see also Eqs. (4.4) and (4.5).

where $\hat{p}|p\rangle = p|p\rangle$, whereas for the mixed state of Eq. (4.2) one has

$$P_\rho(p) = \langle p|\rho|p\rangle = \frac{e^{-p^2}}{\sqrt{\pi}} \tag{4.5}$$

The two probability distributions are different, which means that the measurement of $\hat{p}$ can indeed be used to discriminate $|\alpha_+\rangle$ from Eq. (4.2). However, the difference is due to the oscillatory term in Eq. (4.4), whose oscillation frequency increases with increasing α. Detecting this oscillation therefore requires a precision in the $\hat{p}$ measurement that increases with α, see also Fig. 4.1. In fact, this was one of the examples mentioned in Ref. [6] in order to argue for the plausibility of the considered conjecture. The same effect can also be discussed in terms of the Wigner function [14]. Fig. 4.1 could also be compared to Fig. 2 of Ref. [6], which shows a similar effect for a different macroscopic quantum state.

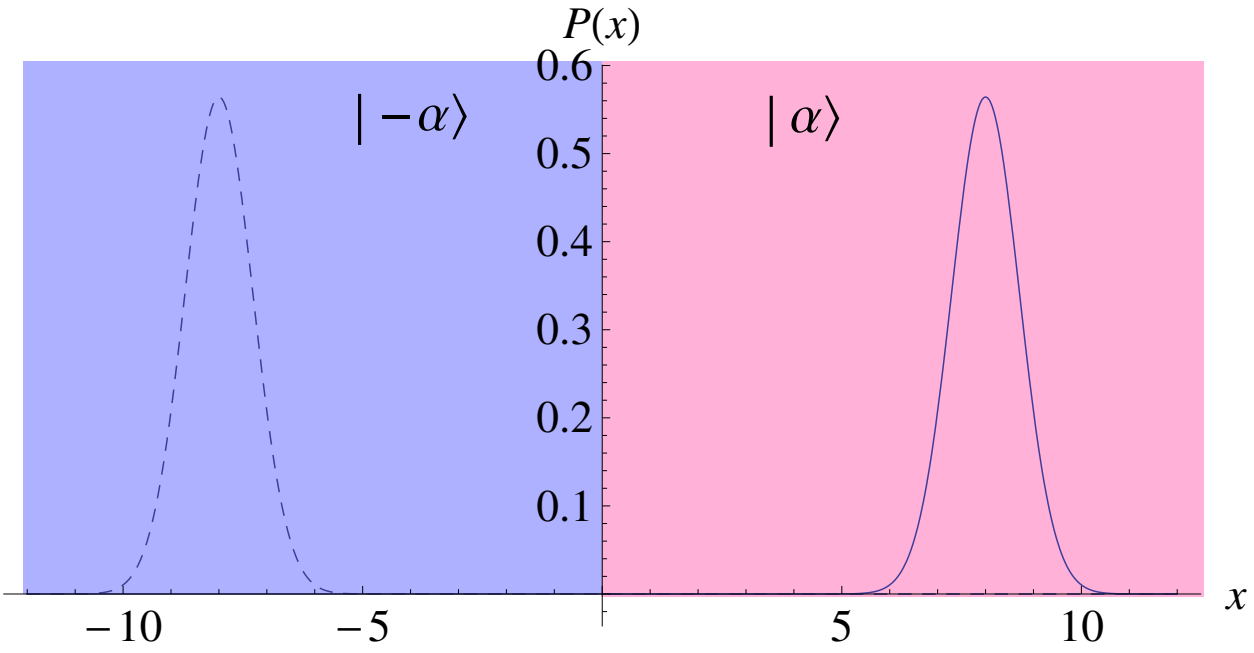

Figure 4.2: Outcome distributions for measurements of the $\hat{x}$ quadrature for the states $|\alpha\rangle$ (solid) and $|-\alpha\rangle$ (dashed) for $\alpha = 8$. For large enough α, the two states can be distinguished by a very coarse measurement. Positive values (red) of $\hat{x}$ can be assigned to $|\alpha\rangle$ and negative values (blue) to $|-\alpha\rangle$. The overlap between the two distributions, and thus the error of this measurement scheme, is negligible.

4.4 Nonlinear rotations of coherent-state qubits: requirement for high control precision

There is a different approach to proving the superposition character of $|\alpha_+\rangle$, which is closely linked to the proposal of Ref. [9]. One can view the states $|\alpha\rangle$ and $|-\alpha\rangle$ as the computational basis states of a "coherent state qubit" [15, 16]. Measurements in the computational basis, which we will also refer to as σ_z measurements (where $\sigma_z = |\alpha\rangle\langle\alpha| - |-\alpha\rangle\langle-\alpha|$), can clearly be done in a very coarse way, e.g. by measuring $\hat{x}$. For large enough α, positive (negative) values correspond to the state $|\alpha\rangle$ ($|-\alpha\rangle$) with extremely high fidelity, and coarse-graining the x values only has a negligible effect on the measurement fidelity, see also Fig. 4.2.

As before, proving the quantum character of $|\alpha_+\rangle$ requires at least one other measurement

that does not commute with σ_z. A natural choice from the qubit perspective is

$$\sigma_y = |\alpha_+\rangle\langle\alpha_+| - |\alpha_-\rangle\langle\alpha_-|, \tag{4.6}$$

where $|\alpha_-\rangle = \frac{1}{\sqrt{2}}(i|\alpha\rangle + |-\alpha\rangle$. If σ_y can be measured, then it is obviously easy to prove that a given source produces the state $|\alpha_+\rangle$ - the corresponding measurement will always give the result $+1$ and never -1, whereas for the mixed state (4.2) the results would be 50/50.

The required measurement of σ_y can be implemented using a Kerr non-linearity, see also Ref. [16]. Changing the sign of α in Eq. (4.1) one has $e^{-i\frac{\pi}{2}\hat{N}^2}|-\alpha\rangle = e^{-i\frac{\pi}{4}}|\alpha_-\rangle$. Inverting these relations one sees that the Kerr operation allows one to rotate the σ_y eigenstates into the σ_z eigenstates, i.e.

$$U|\alpha_+\rangle = |\alpha\rangle, U|\alpha_-\rangle = |-\alpha\rangle, \tag{4.7}$$

where

$$U = e^{-i\frac{\pi}{4}} e^{i\frac{\pi}{2}\hat{N}^2}. \tag{4.8}$$

This means that a measurement of σ_y can be done on an arbitrary state by first applying the rotation U, followed by a measurement in the σ_z basis, as shown in Fig. 4.3. As mentioned before and in Fig. 4.2, the σ_z measurement can be done in a very coarse way. This means that it is possible to prove the presence of the macroscopic superposition using measurements that are coarse in terms of outcome resolution.

However, we argue that it is physically important to also consider the necessary control precision. The control parameter that we focus on here is the phase of the Kerr rotation U. Suppose that instead of exactly $\frac{\pi}{2}$ this phase is $\frac{\pi}{2} + \phi$. Then, when trying to perform the σ_y measurement, the state $|\alpha_+\rangle$ will be rotated not into $|\alpha\rangle$, but into $e^{i\phi\hat{N}^2}|\alpha\rangle$, and $|\alpha_-\rangle$ into $e^{i\phi\hat{N}^2}|-\alpha\rangle$. For simplicity let us consider a Gaussian distribution for ϕ with a width $\sigma \ll 1$ (which is the relevant regime, as will become clear below). Then the final state corresponding to $|\alpha_+\rangle$ is

$$C_\sigma(|\alpha\rangle\langle\alpha|) = \frac{1}{\sqrt{2\pi}\sigma}\int_{-\infty}^{\infty} d\phi e^{-\frac{1}{2}\frac{\phi^2}{\sigma^2}} e^{i\phi\hat{N}^2}|\alpha\rangle\langle\alpha|e^{-i\phi\hat{N}^2} =$$

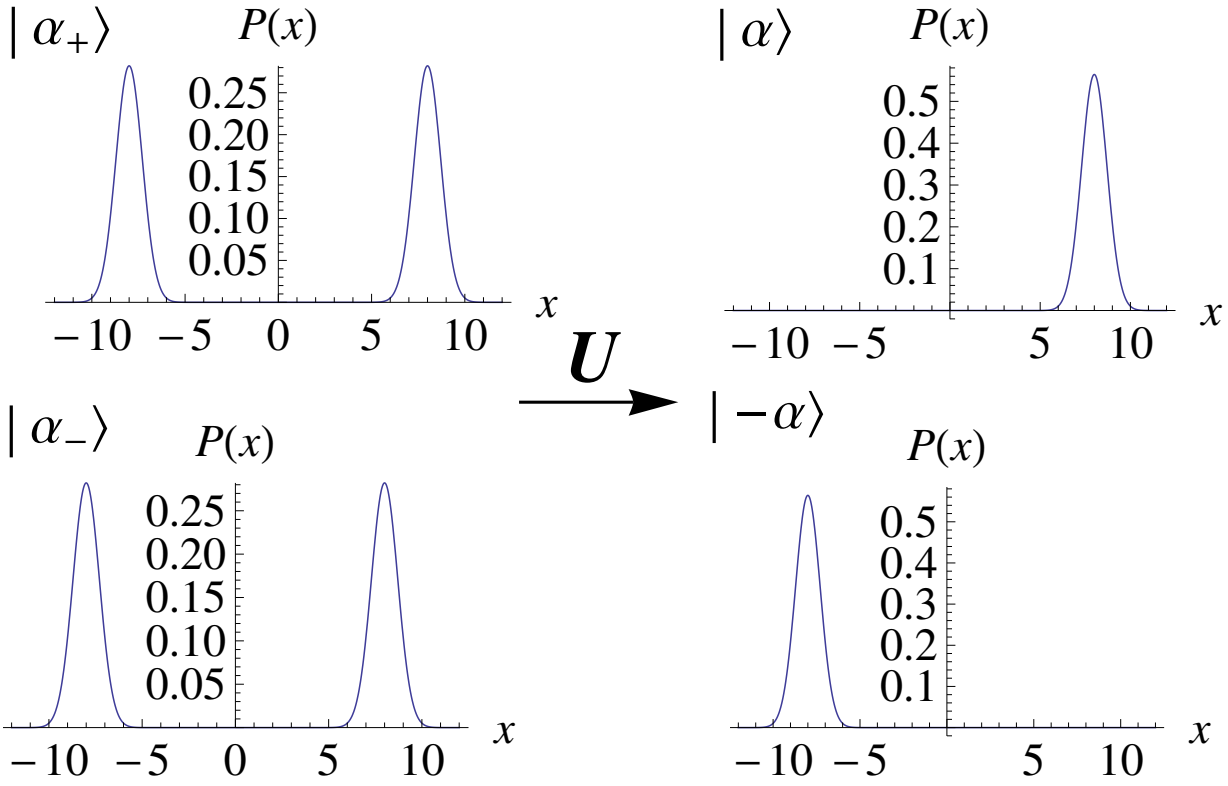

Figure 4.3: The $\hat{x}$ quadrature distributions for the states $|\alpha_+\rangle = \frac{1}{\sqrt{2}}(|\alpha\rangle + i|-\alpha\rangle$ (top left) and $|\alpha_-\rangle = \frac{1}{\sqrt{2}}(i|\alpha\rangle + |-\alpha\rangle$ (bottom left) are identical. However, application of the Kerr rotation Eq. (4.8) transforms $|\alpha_+\rangle$ into $|\alpha\rangle$ (top right) and $|\alpha_-\rangle$ into $|-\alpha\rangle$ (bottom right). These states can now be distinguished by a coarse measurement as in Fig. 4.2.

$$\frac{e^{-\alpha^2}}{\sqrt{2\pi}\sigma}\int_{-\infty}^{\infty}d\phi e^{-\frac{1}{2}\frac{\phi^2}{\sigma^2}}\sum_{n,n'=0}^{\infty}e^{i\phi(n^2-n'^2)}\frac{\alpha^{n+n'}}{\sqrt{n!}\sqrt{n'!}}|n\rangle\langle n'|, \tag{4.9}$$

where we have introduced the notation C_σ for the associated error channel, extended the range of integration for ϕ to infinity (which can be done with negligible error for $\sigma \ll 1$), and expanded $|\alpha\rangle$ in terms of photon number states. Performing the integration over ϕ one finds

$$C_\sigma(|\alpha\rangle\langle\alpha|) = e^{-\alpha^2}\sum_{n,n'=0}^{\infty}e^{-\frac{1}{2}\sigma^2(n^2-n'^2)^2}\frac{\alpha^{n+n'}}{\sqrt{n!}\sqrt{n'!}}|n\rangle\langle n'|. \tag{4.10}$$

The term containing σ leads to a suppression of the off-diagonal elements in the number state basis. The key point for the present work is that this suppression happens faster for larger values of α. This can be seen by remembering that the number distribution for a coherent state is a Poissonian with a peak at α^2 (and a corresponding width α). For large enough α one can then approximate the factor $(n^2 - n'^2)^2 = (n + n')^2(n - n')^2$ in the exponential in Eq. (4.10) by $4\alpha^4(n - n')^2$. This shows that the off-diagonal elements are suppressed by a Gaussian factor $e^{-2\sigma^2\alpha^4(n-n')^2}$. This means that for $\sigma\alpha^2$ the state (4.10) is essentially diagonal in the number basis. Moreover the state corresponding to $|\alpha_-\rangle$, which we denote $C_\sigma(|-\alpha\rangle\langle-\alpha|)$, converges to the same diagonal form. In this regime there is therefore no way to distinguish these two states, see also Fig. 4.4.

This means that the described procedure for measuring σ_y breaks down for phase errors σ that are of order $\frac{1}{\alpha^2}$, or $\frac{1}{N}$, if $N = \alpha^2$ is used to denote the typical number of particles in the system. The precision with which ϕ has to be controlled thus increases with system size. The coherent state qubit approach relies on being able to confine the dynamics of the system to the two-dimensional subspace spanned by $|\alpha\rangle$ and $|-\alpha\rangle$, even though the number of Fock states that effectively contribute to the dynamics is of order α (due to the Poisson distribution of numbers for coherent states). This becomes more and more difficult for increasing α. The evolution of coherent states under small Kerr rotations is discussed also in different terms in Refs. [17, 18].

This result holds no matter how the final measurement in the σ_z basis is performed. For

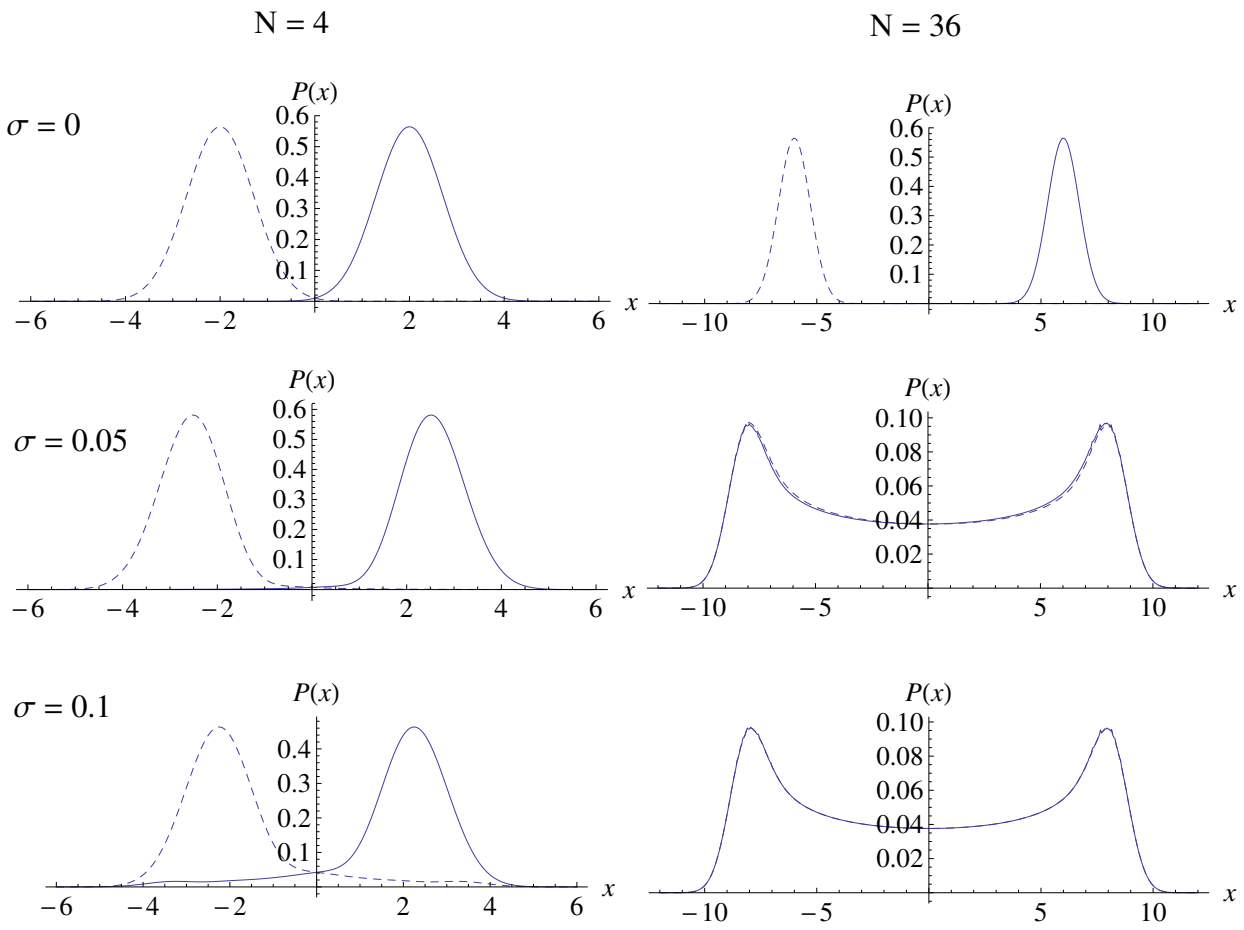

Figure 4.4: Outcome distributions for $\hat{x}$ quadrature measurements for the states $C_\sigma(|\alpha\rangle\langle\alpha|)$ (solid) and $C_\sigma(|-\alpha\rangle\langle-\alpha|)$ (dashed) that are created from the states $|\alpha_+\rangle$ and $|\alpha_-\rangle$ by a Kerr rotation with Gaussian phase uncertainty σ, see Eq. (4.9). We show the case $N = \alpha^2 = 4$ on the left and $N = 36$ on the right, with σ increasing from top to bottom. One sees that the distributions overlap much faster for greater N, leading to errors in the σ_y measurement of Fig. 4.3, see also Fig. 4.2. For large enough σ it becomes impossible to distinguish the two states.

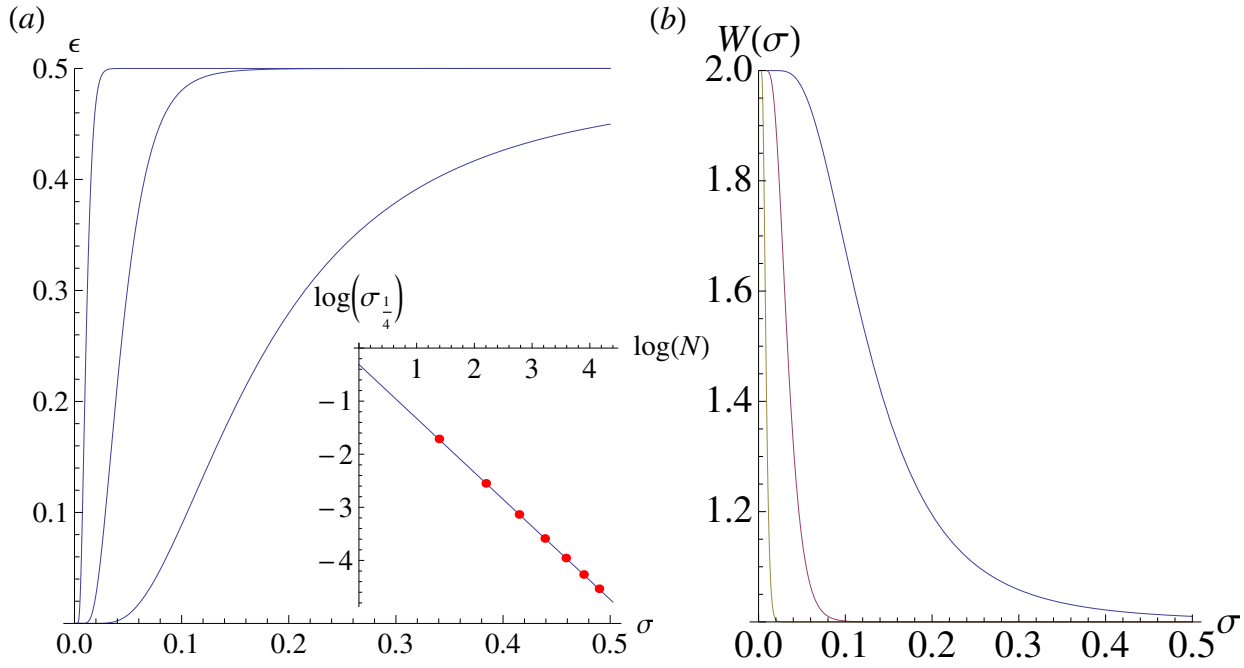

Figure 4.5: (a) The bit-flip error ϵ in the σ_y measurement of Fig. 4.3 as a function of the Kerr phase uncertainty σ, for the cases $N = \alpha^2 = 4, 16, 64$ from bottom to top. One sees that ϵ approaches $\frac{1}{2}$ for increasing σ, and this happens faster for greater N. The log-log plot in the inset shows that the value of σ for which $\epsilon = \frac{1}{4}$ (i.e. half its asymptotic value) scales like $\frac{1}{N}$, as expected from the analytical argument given in the text. (b) Expectation value of the entanglement witness W of Eq. (4.12) for the state of Eq. (4.11), for $N = \alpha^2 = 4, 16, 64$ from top to bottom. For increasing σ the value of W approaches 1 (the bound for separable states), due to the bit-flip errors in the σ_y measurement shown in (a). This happens faster for greater values of N.

concreteness, we show in Figs. 4.4 and 4.5(a) how the phase error σ affects the measurement strategy described in Figs. 4.3 and 4.2. Fig. 4.4 shows that the $\hat{x}$ quadrature distributions for the states $C_\sigma(|\alpha\rangle\langle\alpha|)$ and $C_\sigma(|-\alpha\rangle\langle-\alpha|)$ begin to overlap for increasing σ, and that this happens much faster for greater values of α. Fig. 4.5(a) shows the resulting bit-flip error ϵ for the σ_y measurement of Fig. 4.3. This can be calculated as $\epsilon = \int_{-\infty}^{0} dx\, P(x)$, with $P(x)$ the $\hat{x}$ quadrature distribution for the state $C_\sigma(|\alpha\rangle\langle\alpha|)$. As expected from the above discussion, ϵ approaches $\frac{1}{2}$ (corresponding to complete indistinguishability of the two states) for increasing σ, and this happens faster for greater values of α.

4.5 Macroscopic entanglement

So far we have discussed macroscopic superposition states. We now turn to the detection of macroscopic entanglement. Consider the state

$$|\Phi_-\rangle = \frac{1}{\sqrt{2}}(|\alpha\rangle|\alpha\rangle - |-\alpha\rangle|-\alpha\rangle), \tag{4.11}$$

where the relative sign between the two terms is chosen for convenience. This state can be created, for example, using a Kerr non-linearity, combined with a beam splitter and phase space displacements [10, 16, 19]. Again our focus here is not on how to create the state, but on whether its entanglement can be demonstrated by coarse measurements.

As before, coarse quadrature measurements alone are not sufficient, but the coherent state qubit approach using the Kerr nonlinearity can be applied to the present case as well. Again measurements only in the computational basis (σ_z) are not sufficient to distinguish the entangled state (4.11) from a separable state, in particular from the 50/50 mixture of the product states $|\alpha\rangle|\alpha\rangle$ and $|-\alpha\rangle|-\alpha\rangle$. However, the entanglement can be demonstrated using the witness operator

$$W = \sigma_y \otimes \sigma_y + \sigma_z \otimes \sigma_z. \tag{4.12}$$

One easily verifies that $\langle\Phi_-|W|\Phi_-\rangle = 2$, whereas the modulus of the mean value of W for separable states is bounded by one. This follows from the fact that for any state $|\chi\rangle$ the

norm of the two-dimensional vector $\{\langle\chi|\sigma_y|\chi\rangle, \langle\chi|\sigma_z|\chi\rangle\}$ is bounded by one. For any product state, the mean value of W is the scalar product of two such vectors, and its modulus is therefore also bounded by one; and every separable state is a convex combination of product states, thus satisfying the same bound, see also Ref. [20].

By performing measurements of σ_z and σ_y on each subsystem one can therefore prove the entanglement in the state (4.11). As discussed above, a coarse measurement of the $\hat{x}$ quadrature, for example, is sufficient to do the σ_z measurement, but the σ_y measurement requires moreover the Kerr rotation (4.8). Therefore the exact same control precision requirements as above apply here as well. We showed in Fig. 5(a) that for a phase error $\sigma\frac{1}{\alpha^2}$, the bit-flip error ϵ in the σ_y measurement approaches $\frac{1}{2}$. The measured mean value of W, which is equal to $1 + (1-2\epsilon)^2$ (as can easily be shown, assuming that the σ_z measurement is perfect), therefore tends to 1, see also Fig. 4.5(b). This means that the macroscopic entanglement becomes increasingly hard to detect as α increases. Note that as long as the mean value is greater than one, entanglement can in principle be proven. Our main point here is the scaling with α. Due to this scaling, for any given non-zero level of experimental imperfection, there is a system size above which entanglement is no longer measurable.

4.6 Conjecture and discussion

We have seen that using macroscopic "coherent state qubits" one can in principle observe macroscopic quantum features such as superposition and entanglement using measurements that are very coarse in terms of outcome precision. However, there is a price to be paid. The measurements rely on being able to perform a rotation of the macroscopic qubit basis. When this rotation is implemented using a Kerr non-linearity, the control precision of the Kerr phase shift has to increase with the size of the system. The apparent counter-example of Ref. [9] has thus led us to a refined formulation of the conjecture of Ref. [6] that is both more precise and more general: the measurement precision required for demonstrating macroscopic

quantum effects seems to increase with the size of the system, provided that both outcome precision and control precision are taken into account. This could be compared, for example, to the results of Ref. [21], which studied the effect of coarse graining on macroscopic realism as defined by Leggett [22] and emphasized the computational complexity (rather than the precision) of the operations that were required to observe violations of macroscopic realism.

The above conjecture is attractive, but it is far from proven. Different parts of our argument have a different degree of generality. The requirement for a rotation from a macroscopic superposition basis to a "computational" basis is very general in the present context. On the one hand, for a coarse measurement approach to work there has to be one basis for which the relevant states are easy to distinguish. On the other hand, to prove quantum characteristics one also has to be able to measure at least one observable that corresponds to a different basis, hence the need for a rotation between that basis and the computational basis. As a simple extension, one might want to consider other superposition states or entangled states using the same coherent-state qubits. Proving superpositions or entanglement then requires slightly different rotations. More general qubit basis rotations can be constructed out of the Hadamard-type rotation U of Eq. (4.8) and phase space displacements [16]. The same control precision requirements apply for this construction. They also apply to the measurements proposed in Ref. [9].

But could there be other ways of performing the basic Hadamard rotation? Do they necessarily have the same control precision requirements? In fact, it is known that the Kerr non-linearity is not the only possible solution [11]. Higher powers of $\hat{N}^2$ also work. However, by adapting the argumentation around Eqs. (4.9,4.10) to these cases one can easily show that the control precision requirements are only increased in this case. For a Hamiltonian proportional to $\hat{N}^{2k}$ the necessary control precision scales as $\frac{1}{N^{2k-1}}$. So the Kerr non-linearity is optimal at least for this family of possible approaches.

We suggest that the basic difficulty with implementing a macroscopic basis rotation of

the type of Eq. (4.8) stems from the fact that the underlying Hilbert space is very large. In our case the effective Hilbert space dimension is of order α, corresponding to the range of photon numbers that have significant weights for a coherent state. For increasing α it requires more and more fine-tuning to perform a non-trivial operation on the states $|\alpha\rangle$ and $|-\alpha\rangle$, while confining them to the two-dimensional subspace that they span. This may be a generic difficulty for macroscopic quantum systems.

We feel that proving these conjectures and intuitions would be very interesting, as it would significantly advance our understanding of the macroscopic limit of quantum physics. It would possibly be even more interesting if one could find a counter-example, since the latter might provide a promising avenue towards the demonstration of truly macroscopic quantum effects.

This work was supported by AITF and NSERC.

Bibliography

[1] W.H. Zurek, Rev. Mod. Phys. **75**, 715 (2003).

[2] N.D. Mermin, Phys. Rev. D **22**, 356 (1980).

[3] A. Peres, *Quantum Theory: Concepts and Methods* (Klouwer, 2002).

[4] J. Kofler and C. Brukner, Phys. Rev. Lett. **99**, 180403 (2007).

[5] C. Simon and D. Bouwmeester, Phys. Rev. Lett. **91**, 053601 (2003).

[6] S. Raeisi, P. Sekatski, and C. Simon, Phys. Rev. Lett. **107**, 250401 (2011).

[7] N. Spagnolo, C. Vitelli, M. Paternostro, F. De Martini, and F. Sciarrino, Phys. Rev. A **84**, 032102 (2011).

[8] S. Portolan, O. Di Stefano, S. Savasta, F. Rossi, and R. Girlanda, Phys. Rev. A **73**, 020101(R) (2006).

[9] H. Jeong, M. Paternostro, and T.C. Ralph, Phys. Rev. Lett. **102**, 060403 (2009).

[10] R. Ghobadi, S. Raeisi, and C. Simon, arXiv:1206.3673

[11] B. Yurke and D. Stoler, Phys. Rev. Lett. **57**, 13 (1986).

[12] M. Brune *et al.*, Phys. Rev. Lett. **77**, 4887 (1996); C. Monroe, D.M. Meekhof, B.E. King, and D.J. Wineland, Science **272**, 1131 (1996); M.W. Noel and C.R. Stroud, Jr., Phys. Rev. Lett. **77**, 1913 (1996); A. Auffves *et al.*, Phys. Rev. Lett. **91**, 230405 (2003).

[13] G. Kirchmair *et al.*, Nature **495**, 205 (2013).

[14] W.H. Zurek, Nature **412**, 712 (2001).

[15] P.T. Cochrane, G.J. Milburn, and W.J. Munro, Phys. Rev. A **59**, 2631 (1999); W.J. Munro, G.J. Milburn, and B.C. Sanders, Phys. Rev. A **62**, 052108 (2000).

[16] H. Jeong and M.S. Kim, Phys. Rev. A **65**, 042305 (2002).

[17] M. Kitagawa and Y. Yamamoto, Phys. Rev. A **34**, 3974 (1986).

[18] S. Haroche and J.-M. Raimond, *Exploring the Quantum: Atoms, Cavities, and Photons* (Oxford University Press, Oxford, 2006).

[19] B.C. Sanders, Phys. Rev. A **45**, 6811 (1992); B. C. Sanders, J. Phys. A: Math. Theor. **45**, 244002 (2012).

[20] H.S. Eisenberg, G. Khoury, G.A. Durkin, C. Simon, and D. Bouwmeester, Phys. Rev. Lett. **93**, 193901 (2004).

[21] J. Kofler and C. Brukner, Phys. Rev. Lett. **101**, 090403 (2008).

[22] A.J. Leggett, J. Phys. Condens. Matter **14**, R415 (2002).

Chapter 5

Strong entanglement between macroscopic beams via weak cross Kerr-nonlinearties

5.1 Introduction

Vigorous efforts are currently being undertaken to create large entanglement. On one hand, people are trying to create quantum entanglement of macroscopic system. For instance, in Ref.[2] entanglement between photonic qubit states displaced number states with 10^8 photons are created. On the other hand, people are trying to increase the amount of entanglement [1]. In this letter, we are trying to do both of them at the same time. We propose to create strong entanglement involving macroscopic states, by using weak Kerr nonlinearities.

There have been some proposals in which weak Kerr nonlinearities have useful applications in quantum information processing [3, 15]. Weak nonlinearities can be used to build photon-number-resolving QND detectors [14], and with the help of homodyne measurements and classical feedforward elements, can be exploited to construct nearly deterministic cNOT gates [16] and non-destructive Bell state detectors [17]. Recently, there has been major a advancement in creating a cross Kerr phase shift of $10^{-3}rad$ at single photon level via the AC Stark shift [11]. One of the major advantages over previous stronger phase shifts is that in this case the nonlinearities are not easily saturated. This makes creating high dimensional entanglement possible.

In this Chapter, we propose to use weak cross Kerr nonlinearities to create a new class of strong entangled states, which is robust under lossy conditions. The main idea is to amplify the weak cross Kerr phase shift by sending two coherent states, creating macro-macro entanglement. The state is macroscopic in that both the size of the system (mean

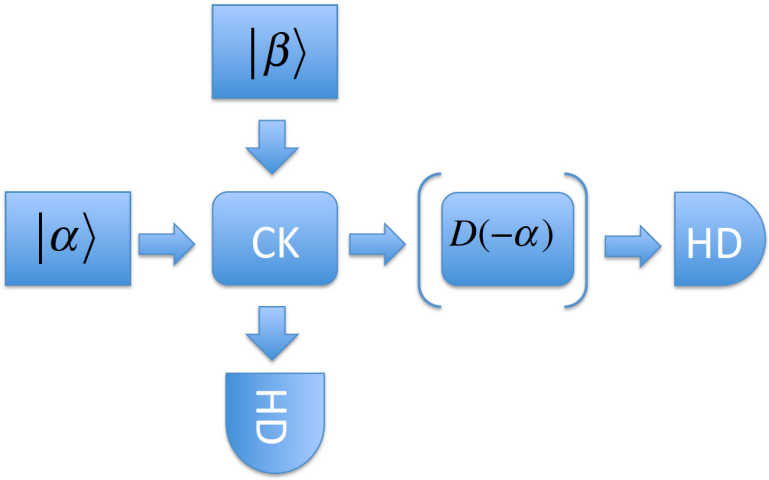

Figure 5.1: Scheme to create and detect macroscopic entanglement

photon number) and the amount of entanglement are very large. Moreover, we show that the entanglement is robust under photon loss, the main source of decoherence. This strong entanglement also have the potential to be verified experimentally.

It should be noted that this project is still in process. What we present here is some preliminary results. We hope the project will be finished soon.

5.2 Strong entanglement

We send two coherent states into a Cross Kerr medium,

$$|\psi\rangle = |\alpha\rangle_1|\beta\rangle_2 = ||\alpha|e^{i|\beta|^2\phi}\rangle_1||\beta|e^{i|\alpha|^2\phi}\rangle_2, \tag{5.1}$$

where the phases are defined to cancel the rotational effect of the Kerr evolution so that their Wigner functions center at $(|\alpha|(|\beta|), 0)$ in phase space. We will omit the subscribes when their are obvious. After cross Kerr evolution with a small phase shift θ, the state becomes

$$e^{-i\hat{n}_1\hat{n}_2\theta}|\psi\rangle = \sum_{n=0}^{\infty} e^{-\frac{|\alpha|^2}{2}}\frac{\alpha^n}{\sqrt{n!}}|n\rangle_1|\beta e^{-in\theta}\rangle_2 = \sum_{n=0}^{\infty} e^{-\frac{|\beta|^2}{2}}\frac{\beta^n}{\sqrt{n!}}|\alpha e^{-in\theta}\rangle_2|n\rangle_1. \tag{5.2}$$

As we know, the overlap of coherent states with different phases are

$$|\langle\beta e^{-in\theta}|\beta e^{-im\theta}\rangle|^2 = e^{-2|\beta|^2(1-cos((m-n)\theta))} \approx e^{-(|\beta|\theta(m-n))^2}. \tag{5.3}$$

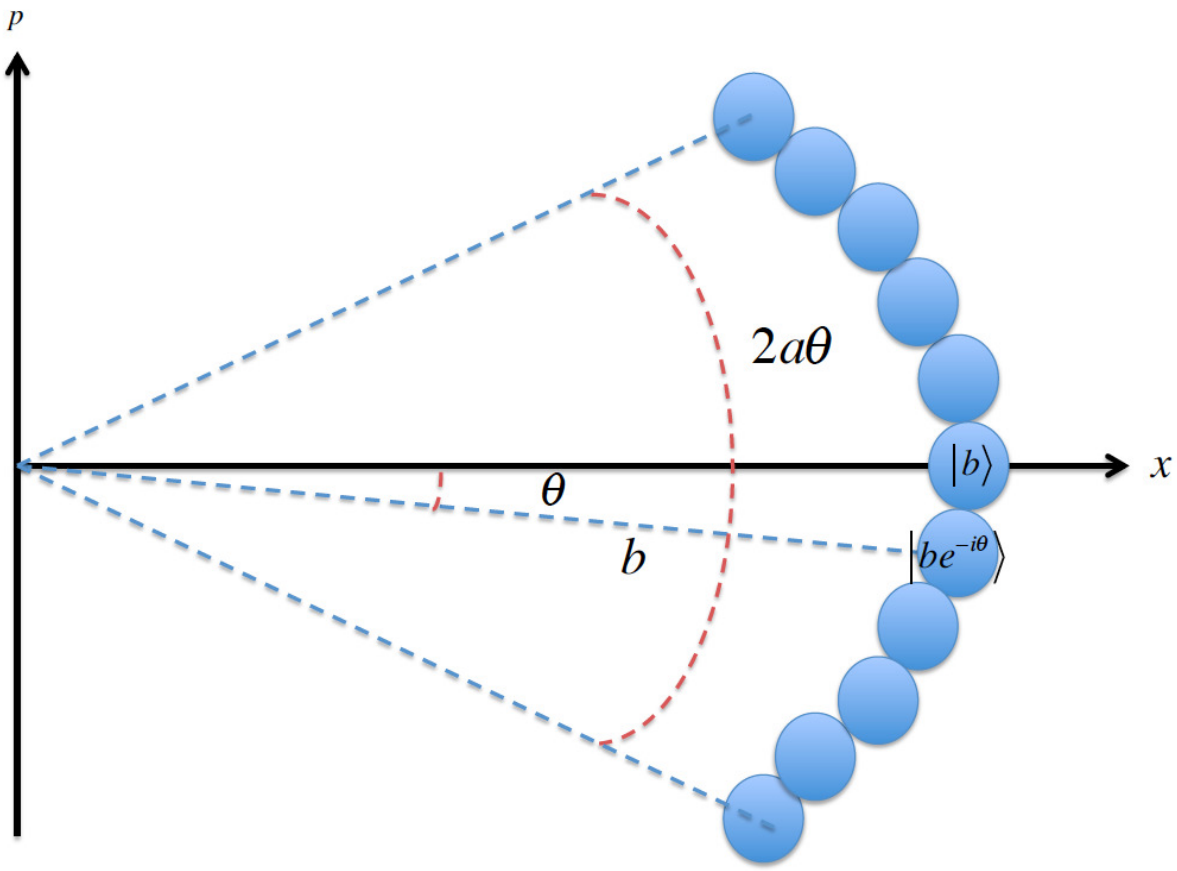

Figure 5.2: The structure of the state

When $|\beta|\theta \geq 2$, these coherent states with various n, m are well separated in phase space, as shown in 5.2, so that they could be treated as quasi-orthogonal. This indicates that the photon number on one side and phase on the other side are entangled.

In the pure case, the entanglement can be quantified by von Neumann entropy (VNE). In Fig. (5.3) we show the von Neumann entropy for symmetric ($|\alpha| = |\beta| = 5$) and asymmetric cases ($|\alpha| = 5, |\beta| = 40$). It can be seen that for symmetric case the VNE increases very fast and is peaked at around $\theta = 0.31$ for about 2.8. And then it begins to oscillate. This can be understood intuitively as follows. When the phase shift θ increases, coherent states in Eqn. (5.2) with different phases begin to split towards quasi-orthogonality, so that the entanglement increases. When $\theta = 0.31$, adjacent coherent states are already well separated with the overlap $|\langle \beta e^{-in\theta} | \beta e^{-i(n+1)\theta} \rangle|^2 \approx e^{-1.5^2} = 0.085$, so that further separation would not

increase entanglement very much. On the other hand, according to Gaussian distribution, the majority of the fock states is in the range $(|\alpha|^2 - |\alpha|, |\alpha|^2 + |\alpha|)$, so that the angle of phase distribution of coherent states is about $2|\alpha|\theta$. When $\theta \geq 0.31$ the phase distribution is larger than 2π. This means that coherent states from the opposite ends begin to overlap, thus the entanglement decreases. We also shows that with a larger $|\beta|$, VNE increases to peak value much faster. This is because that the overlap of adjancent coherent states are determined by $|\beta|\theta$ as shown in Eqn.5.3 . In general, the maximum of VNE is bounded by the smaller one of $|\alpha|$ and $|\beta|$, since the number of the components in 5.2 is about $2|\alpha|$, and the entanglement will not increase much after the coherent states in the second beam are well separated. As the overlap of coherent states depends on $|\beta|\theta$, increasing $|\beta|$ enables us to achieve maximum entanglement with smaller phase shift, yet it would not significantly increase the dimension of entanglement.

It is obvious that one can in principle create very high entanglement with very small Kerr phase shift by sending two strong coherent beam, for example $|\alpha| = |\beta| = 1000, \theta = 1.6 * 10^{-3}$. However, to experimentally verify such entanglement would be challenging, as discussed later. We would mainly analyze the case when $|\alpha| = 5$, which is feasible for current technology. Here the entanglement is macroscopic in two sense. Firstly, the amount of entanglement is large. As shown in 5.3 the VNE is 3.1 ebit, and the dimension of entanglement is 32 (see supplementary). Secondly, the average photon number of two entangled beams are large, one 25 and the other one can be millions of photons.

There is a better way to quantity the entanglement, the quantum purity, which can be obtained analytically. For symmetric cases when $\alpha = \beta$, the purity (details see Appendix)

$$Tr(\rho^2) = e^{-4a^2} \sum_{m,n,k,l=0}^{\infty} \frac{\alpha^{2(m+n+k+l)}}{n!m!k!l!} e^{i(m-n)(k-l)\theta} \tag{5.4}$$

In the limit when $\alpha \gg 0$, the above summations can be approximated as Gaussian integrations. After some algebra the result reduces to

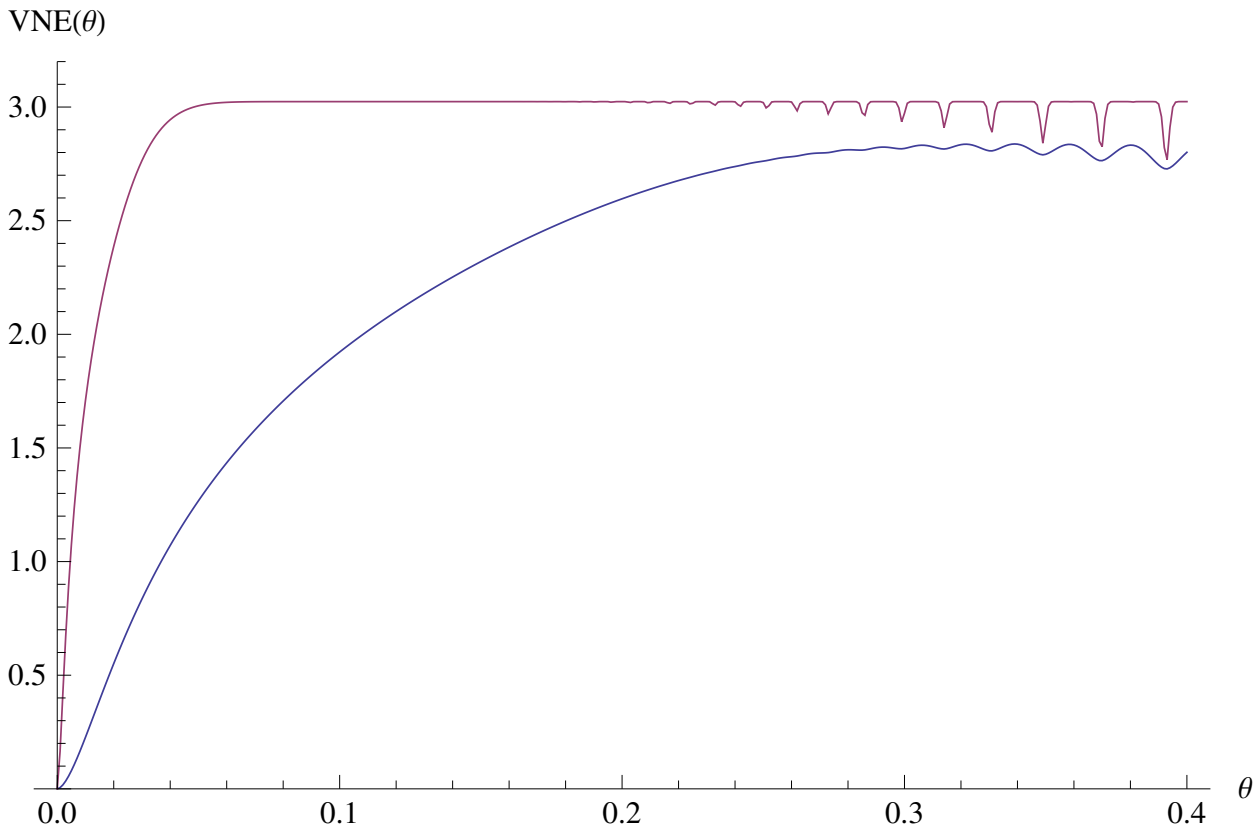

Figure 5.3: Von Neumann Entropy for symmetric (lower, $|\alpha| = |\beta| = 5$) and asymmetric (upper, $|\alpha| = 5, |\beta| = 40$) cases.

$$Tr(\rho^2) = \frac{1}{\sqrt{1+4a^4\theta^2}} \tag{5.5}$$

We define $D(\rho) = 1/Tr(\rho^2) = \sqrt{1+4a^4\theta^2}$, which is the lower bound of the dimension of the entanglement. This can be understood as follows. As we know, every bipartite pure states has a unique Schimidt decomposition

$$|\phi\rangle = \sum_{n=0}^{m} C_n |n\rangle|n\rangle \tag{5.6}$$

The dimension of the entanglement is m, the number of components in such a decomposition. It can be shown that for a given purity, the smallest dimension m is obtained when the state is maximally entangled (all C_n are the same so that $P_n = |C_n|^2 = 1/m$). We thus have

$$D(\rho) = 1/Tr(\rho^2) = 1/\sum_{n=0}^{m} |C_n|^4 = 1/\sum_{n=0}^{m} {P_n}^2 = m \tag{5.7}$$

When the state with the same dimension is not maximally entangled, it is obvious that $m > D(\rho) = 1/\sum_{n=0}^{m} {P_n}^2$. This is why it is the lower bound of the dimension of the entanglement.

It can be shown in Fig.5.4 that the amount entanglement is very high with a cross Kerr phase shift as small as $10^{-3} rad$.

5.3 Robust under Decoherence

An interesting question is how such strong entanglement behaves under decoherence. Here we show that it is robust under decoherence. The major decoherence in this case is the photon loss during the creation and detection of the entanglement. Here we focus on the latter, as the former can be controlled quite well [11]. Using the beam splitter model to deal with photon loss, one have $|\alpha\rangle|0\rangle \rightarrow |t\alpha\rangle|r\alpha\rangle$, where $t^2+r^2 = 1$ and the second channel is the loss channel. Since the loss after the Kerr effect is a local operation that does not influence

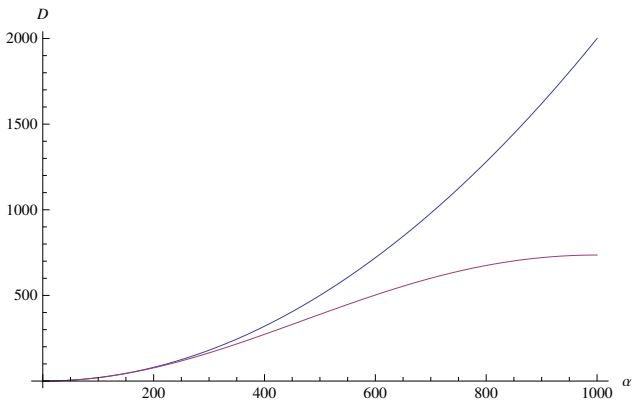

Figure 5.4: $D(\rho)$ (red) and $W(\rho)/2$ with no loss (blue) as the function of the size of the system a for $10^{-3} rad$ cross Kerr phase shift. It can be seen that for $a = 1000$ the entanglement is about 2000 dimensions. Moreover, for $a < 200$ our witness matches the dimension of entanglement very well.

the entanglement, we can treat the loss in two beams independently and significantly simplify the calculation.

We first treat the loss in the second beam by adding a loss channel, and then expand the coherent states in the second and third beam and recombine the terms to make the first channel a coherent state $\sum_{n=0}^{\infty} e^{-\frac{|\alpha|^2}{2}} \frac{\alpha^n}{\sqrt{n!}} |n\rangle |\beta e^{-in\theta}\rangle |0\rangle \rightarrow \sum_{n=0}^{\infty} e^{-\frac{|\alpha|^2}{2}} \frac{\alpha^n}{\sqrt{n!}}{}_n |n\rangle |t_2 \beta e^{-in\theta}\rangle |r_2 \beta e^{-in\theta}\rangle$
$= \sum_{m,k=0}^{\infty} |\alpha e^{-i(m+k)\theta}\rangle e^{-\frac{|\beta|^2}{2}} \frac{(t_2\beta)^m}{\sqrt{m!}} |m\rangle \frac{(r_2\beta)^k}{\sqrt{k!}} |k\rangle$

Now we treat the loss in the first beam by adding another loss channel:

$$|\psi\rangle \rightarrow \sum_{m,k=0}^{\infty} |t_1 \alpha e^{-i(m+k)\theta}\rangle_1 |r_1 \alpha e^{-i(m+k)\theta}\rangle_3 e^{-\frac{|\beta|^2}{2}} \frac{(t_2\beta)^m}{\sqrt{m!}} |m\rangle_2 \frac{(r_2\beta)^k}{\sqrt{k!}} |k\rangle_4 \tag{5.8}$$

Here the channel 3 and 4 are the loss channels. Here it is clear that the entanglement between channel 1 and 2 leaks into channel 3 and 4. Tracing out the loss channels we obtain the reduced density matrix

$\rho = \sum_{m,m',n,n'}^{\infty} \frac{(t_1\alpha)^m (t_1\alpha^*)^{m'} (t_2\beta)^n (t_2\beta^*)^{n'}}{\sqrt{m!m'!n!n'!}} \exp(-i(mnm'n')\theta)$
$\exp(-(r_1|\alpha|)^2(1 - e^{-i(m-m')\theta}) - (r_2|\beta|)^2(1 - e^{-i(n-n')\theta}))|m\rangle\langle m'| \otimes |n\rangle\langle n'|$

It is clear that the off-diagonal terms will decrease with loss, and thus the entanglement decreases.

We can quantify the entanglement by numerically calculating the Logarithmic Negativity

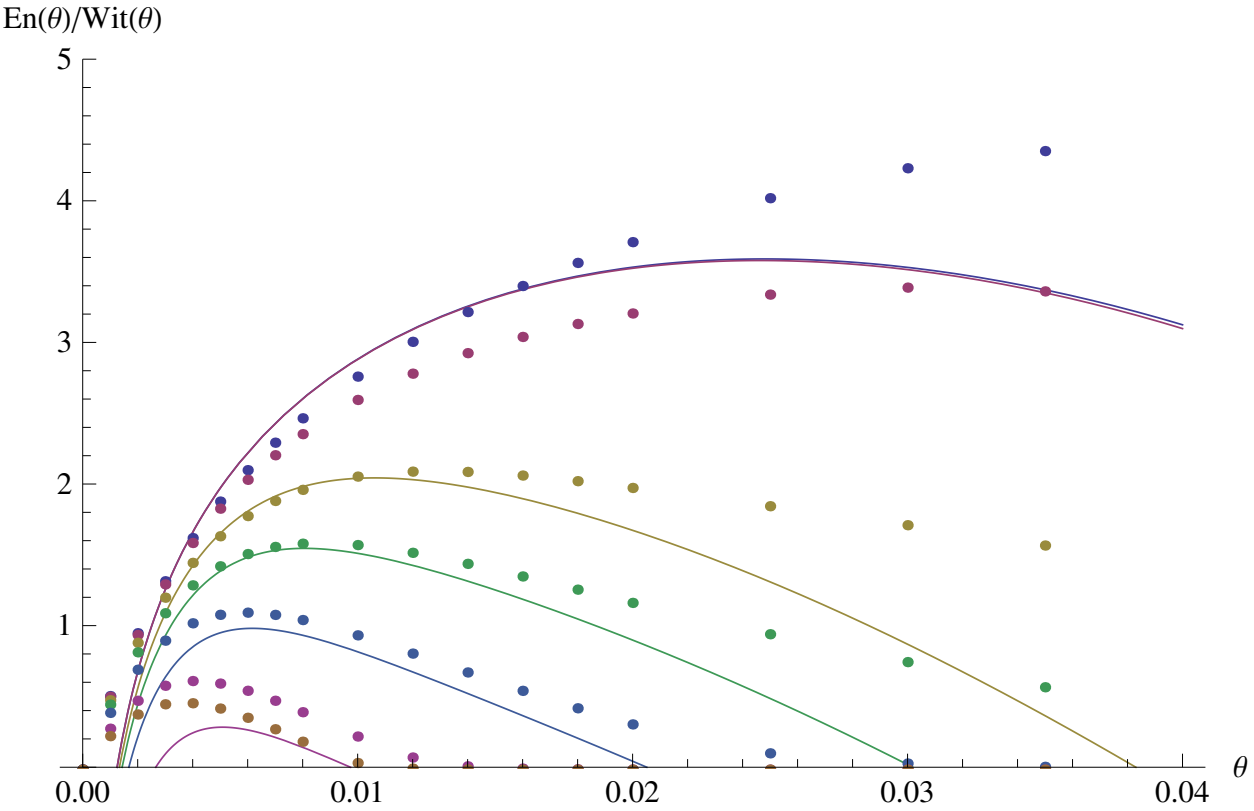

Figure 5.5: Logarithmic Negativity (dotted) and witness (continuous) as a function of phase shift θ for $|\alpha| = 5, |\beta| = 40$ with various loss rate. The loss rate is $0, 1\%, 5\%, 10\%, 20\%, 40\%, 50\%$ from top to bottom.

(En)

$$En(\rho) = Log_2||\rho^{T_A}||_1 \tag{5.9}$$

Here ρ^{T_A} means partial transpose. In Fig. 5.5we show En as a function of phase shift θ for $|\alpha| = 5, |\beta| = 40$ with various loss rate. Here we assumed that the loss rate of the two modes are the same for simplicity (we analyzed the cases when they are not the same in Appendix). In the pure case ($r = 0$). It can be shown that the entanglement is robust under photon loss. However, with larger loss rate the maximum entanglement decreases, which matches the intuition that the larger the entanglement is, the more sensitive it is to decoherence. Moreover, the θ to achieve maximum En also turns to be smaller for larger loss.

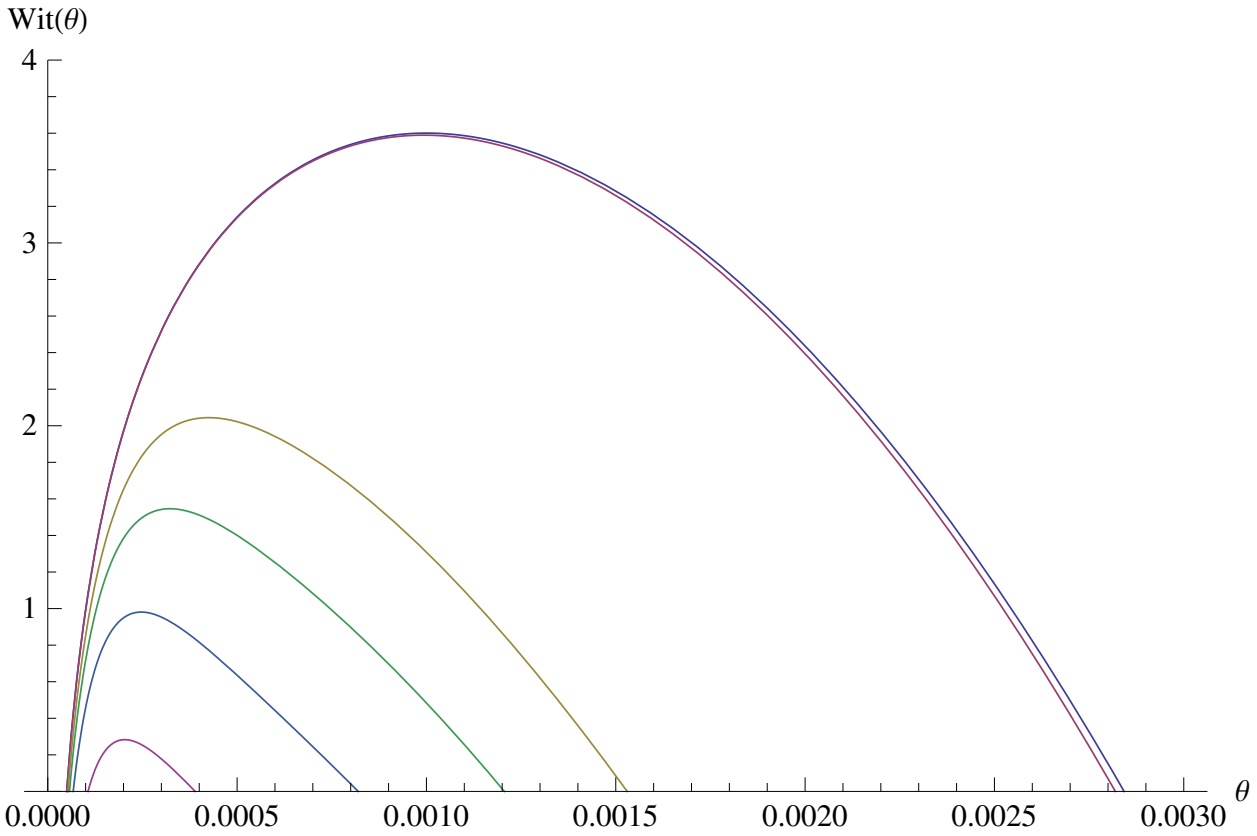

Figure 5.6: Witness as a function of phase shift θ for $|\alpha| = 5, |\beta| = 1000$ with various loss rate.The loss rate is $0, 1\%, 5\%, 10\%, 20\%, 40\%, 50\%$ from top to bottom. It can be seen that the maximum does not change compared to the previous case , however the θ to obtain maximum is much smaller. With 5% loss the maximum is 2.1 at $\theta = 4 * 10^{-4}$.

We can in principle calculate En for much larger states, for example $|\beta| = 1000$, so that we can get a very large entanglement, however the computational resources required are tremendous. This means that we have to develop our own entanglement witness to prove that our state is still entangled under lossy condition.

By looking at the structure of the original state in Eq.5.2, we found that the photon number in mode one times θ plus the phase of the second mode is zero, and the photon number in mode two times θ plus the phase of the first mode is zero, which is similar to the EPR correlations

$$\hat{x}_1 + \hat{x}_2 = 0, \hat{p}_2 - \hat{p}_1 = 0$$

We can develop a similar entanglement witness to the Duan's witness [10] if there are well-defined phase operators. Since there are not, we have to use more complicated operators that have similar relations. Fortunately, we found that the average value of the operator $\hat{o} = |\alpha| \sin((\hat{n}_2 - |\beta|^2)\theta) + \hat{p}_1$ is zero

$$\begin{aligned} \langle \hat{o} \rangle &= \sum_{n=0}^{\infty} e^{-|\beta|^2} \frac{|\beta|^{2n}}{n!} (\left\langle n||\alpha| \sin((\hat{n}_2 - |\beta|^2)\theta)|n \right\rangle + \left\langle \alpha e^{-in\theta} |\hat{p}_1| \alpha e^{-in\theta} \right\rangle) \\ &= \sum_{n=0}^{\infty} e^{-|\beta|^2} \frac{|\beta|^{2n}}{n!} (|\alpha| \sin((n - |\beta|^2)\theta) + |\alpha| \sin((|\beta|^2 - n)\theta)) = 0 \end{aligned}$$

When there is loss, in each of the term in Eq. 5.8 $|t_1 \alpha e^{-i(m+k)\theta}\rangle_1 |r_1 \alpha e^{-i(m+k)\theta}\rangle_3 |m\rangle_2 |k\rangle_4$ we only have access to beam 1 and 2. Due to the photon loss, there is a discrepancy of the photon number m in beam 2 and the phase $(m+k)\theta$ in beam 1. To fix this, we noticed that the average of k is $(r_2|\beta|)^2$, and define $\hat{u} = \hat{p}_1 + t_1|\alpha| \sin((\hat{n}_2 - t_2^2|\beta|^2)\theta)$. Now we have

$$\begin{aligned} \langle \hat{u} \rangle &= \sum_{m,k=0}^{\infty} e^{-|\beta|^2} \frac{|t_2\beta|^{2m} |r_2\beta|^{2k}}{m!k!} (\langle t_1 \alpha e^{-i(m+k)\theta} |\hat{p}_1| t_1 \alpha e^{-i(m+k)\theta} \rangle + \left\langle m|t_1|\alpha| \sin((\hat{n}_2 - t_2^2|\beta|^2)\theta)|m \right\rangle) \\ &= \sum_{m,k=0}^{\infty} e^{-|\beta|^2} \frac{|t_2\beta|^{2m} |r_2\beta|^{2k}}{m!k!} (t_1|\alpha| \sin((|\beta|^2 - m - k)\theta) + t_1|\alpha| \sin((m - t_2^2|\beta|^2)\theta)) \end{aligned}$$

which is 0 when there is no loss. Similarly, we define $\hat{v} = \hat{p}_2 + t_2|\beta| \sin((\hat{n}_1 - t_1^2|\alpha|^2)\theta)$. It can be proved that for separable states (see Appendix)

$$\left\langle (\Delta \widehat{u})^2 \right\rangle + \left\langle (\Delta \widehat{v})^2 \right\rangle$$
$$\geq |\langle [\hat{p}_1, t_2|\beta| \sin((\hat{n}_1 - t_1^2|\alpha|^2)\theta)] \rangle| + |\langle [\hat{p}_2, t_1|\alpha| \sin((\hat{n}_2 - t_2^2|\beta|^2)\theta)] \rangle|$$

We thus define the entanglement witness

$$W = Log_2 \frac{|\langle[\hat{p}_1, t_2|\beta| \sin((\hat{n}_1 - t_1^2|\alpha|^2)\theta)]\rangle| + |\langle[\hat{p}_2, t_1|\alpha| \sin((\hat{n}_2 - t_2^2|\beta|^2)\theta)]\rangle|}{(\Delta\hat{u})^2 + (\Delta\hat{v})^2} \tag{5.10}$$

It is obvious that when $W \geq 0$ our state is entangled. We found that our witness matches the En very well, and is usually a lower bound of En in lossy conditions, as shown in Fig. 5.5.

We also found that when we increasing $|\beta|$ we can achieve maximum En for a smaller phase shift θ, and this holds when there is loss. In Fig. 5.6we show En as a function of phase shift θ for $|\alpha| = 5, |\beta| = 1000$ with various loss rate. It can be seen that the maximum does not change very much compared to the previous case when $|\alpha| = 5, |\beta| = 40$, however the required θ to obtain the maximum entanglement is much smaller. With 5% loss the maximum is 2.1 at $\theta = 4 * 10^{-4}$, which is achievable with current technology.

Moreover, as we know, in the pure case, when we increase $|\alpha|$ the entanglement will increase. Unfortunately this does not hold when there is loss. From En and our witness we found that the maximum amount entanglement is bounded by the loss rate. In Fig. 5.7 we shows W as a function of $|\alpha|$ and θ with 10% loss when we fix $|\beta| = 1000$. It can be seen that even though $|\alpha|$ rises to 1000, W is still about 1.6. We tried other loss rates and get similar results, and for En it is the same.

In principle, this witness can be measured by optical homodyne tomography (OHD). For the case when$|\alpha| = 5, |\beta| = 1000$ we displace the second beam towards the origin by $D(-|\beta|)$ so that the average photon number is not too large. We then construct the Wigner function for the displaced state by OHD. The Wigner function of the original states can be obtained by displacing the Wigner function back, basing on which we can obtain the value of the witness.

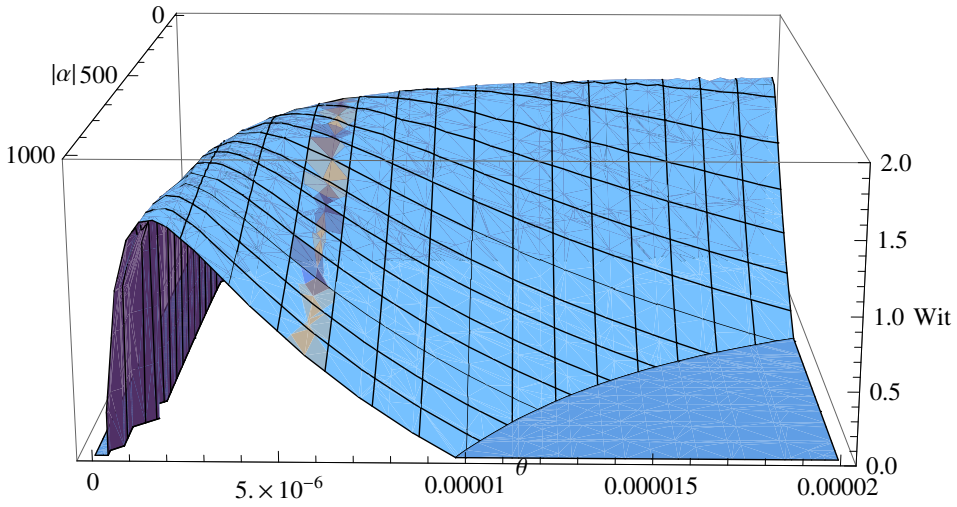

Figure 5.7: Witness as a function of $|\alpha|$ and θ when we fix $|\beta| = 1000$ with 10% loss. It can be seen that even though $|\alpha|$ rises to 1000, W is still about 1.6.

5.4 Appendix

5.4.1 Derivation of the purity

The quantum purity is defined as the trace of the square of the reduced density matrix,

$$Tr(\rho_1^2) = e^{-2(a^2+b^2)} \sum_{m,n,k,l=0}^{\infty} \frac{a^{2(m+n)} b^{2(k+l)}}{n!m!k!l!} e^{i(m-n)(k-l)\theta} \tag{5.11}$$

In the limit when $a, b \gg 0$, the above summations can be approximated as Gaussian integrations. After some algebra the result reduces to

$$Tr(\rho_1^2) = \frac{1}{\sqrt{1+4a^2b^2\theta^2}} \tag{5.12}$$

We define $D(\rho) = 1/Tr(\rho_1^2) = \sqrt{1+4a^2b^2\theta^2}$, which is the lower bound of the dimension of the entanglement. This can be understand as follow. As we know, every bipartite pure states has a unique Schimidt decomposition

$$|\phi\rangle = \sum_{n=0}^{m} C_n |n\rangle |n\rangle \tag{5.13}$$

The dimension of the entanglement is m, the number of components in such decomposition. It can be shown that for a given purity, the smallest dimension m is obtained when

the state is maximally entangled (all C_n are the same so that $P_n = |C_n|^2 = 1/m$). We thus have

$$D(\rho) = 1/Tr(\rho_1^2) = 1/\sum_{n=0}^{m} |C_n|^4 = 1/\sum_{n=0}^{m} {P_n}^2 = m \tag{5.14}$$

When the state with dimension m is not maximally entangled, it is obvious that $m > D(\rho) = 1/\sum_{n=0}^{m} {P_n}^2$. This is why $D(\rho)$ is the lower bound of the dimension of the entanglement.

It can be shown in Fig.3 that the amount entanglement is very high with a cross Kerr phase shift as small as $10^{-3} rad$.

$$\begin{aligned}
Tr(\rho^2) &= e^{-2a^2} \sum_{m,n=0}^{\infty} \frac{a^{2(m+n)}}{n!m!} exp(-2b^2(1 - \frac{exp(i(m-n)\theta) + exp(i(n-m)\theta)}{2})) \\
&= e^{-2(a^2+b^2)} \sum_{m,n=0}^{\infty} \frac{a^{2(m+n)}}{n!m!} exp(b^2 exp(i(m-n)\theta)) exp(b^2 exp(i(n-m)\theta)) \\
&= e^{-2(a^2+b^2)} \sum_{m,n,k,l=0}^{\infty} \frac{a^{2(m+n)}}{n!m!} \frac{(b^2 exp(i(m-n)\theta))^k}{k!} \frac{(b^2 exp(i(n-m)\theta))^l}{l!} \\
&= e^{-2(a^2+b^2)} \sum_{m,n,k,l=0}^{\infty} \frac{a^{2(m+n)} b^{2(k+l)}}{n!m!k!l!} e^{i(m-n)(k-l)\theta}
\end{aligned}$$

In the limit when $a, b \gg 0$, the above summations can be approximated as Gaussian integration

$$Tr(\rho^2) = \frac{1}{2\pi a^2 2\pi b^2} \int dm dn dk dl e^{\frac{-(m-a^2)^2}{2a^2}} e^{\frac{-(n-a^2)^2}{2a^2}} e^{\frac{-(k-b^2)^2}{2b^2}} e^{\frac{-(l-b^2)^2}{2b^2}} e^{i(m-n)(k-l)\theta}$$

let $m - a^2 = p_1, n - a^2 = p_2, k - b^2 = q_1, l - b^2 = q_2$,

$$Tr(\rho^2) = \frac{1}{2\pi a^2 2\pi b^2} \int dp_1 dq_1 dp_2 dq_2 exp(-\frac{p_1^2 + p_2^2}{2a^2}) exp(-\frac{q_1^2 + q_2^2}{2b^2}) e^{i(p_1 - p_2)(q_1 - q_2)\theta}$$

let $x_1 = \frac{p_1 - p_2}{\sqrt{2}}, x_2 = \frac{p_1 + p_2}{\sqrt{2}}, y_1 = \frac{q_1 - q_2}{\sqrt{2}}, y_2 = \frac{q_1 + q_2}{\sqrt{2}}$, then$p_1^2 + p_2^2 = x_1^2 + x_2^2, q_1^2 + q_2^2 = y_1^2 + y_2^2$

$$Tr(\rho^2) = \frac{1}{2\pi a^2 2\pi b^2} \int dx_1 dy_1 dx_2 dy_2 exp(-\frac{x_1^2 + x_2^2}{2a^2}) exp(-\frac{y_1^2 + y_2^2}{2b^2}) e^{2ix_1 y_1 \theta}$$

$$= \frac{1}{2\pi a^2 2\pi b^2}\int dx_2 dy_2 exp(-\frac{x_2^2}{2a^2}-\frac{y_2^2}{2b^2})\int dx_1 dy_1 exp(-\frac{x_1^2}{2a^2}-\frac{y_1^2}{2b^2})e^{2ix_1y_1\theta}$$
$$= \frac{1}{2\pi a^2 2\pi b^2}(2ab\pi)\frac{2\pi ab}{\sqrt{1+4a^2b^2\theta^2}} = \frac{1}{\sqrt{1+4a^2b^2\theta^2}}$$

5.4.2 Proof of the witness

We define

$$\hat{u} = \hat{p}_1 + t_1|\alpha|\sin((\hat{n}_2 - t_2^2|\beta|^2)\theta)$$

$$\hat{v} = \hat{p}_2 + t_2|\beta|\sin((\hat{n}_1 - t_1^2|\alpha|^2)\theta)$$

and we prove as follow that for separable states $(\Delta\hat{u})^2+(\Delta\hat{v})^2 \geq |\langle[\hat{p}_1, t_2|\beta|\sin((\hat{n}_1 - t_1^2|\alpha|^2)\theta)]\rangle|+ |\langle[\hat{p}_2, t_1|\alpha|\sin((\hat{n}_2 - t_2^2|\beta|^2)\theta)]\rangle|$

$$\begin{aligned}
&\left\langle(\Delta\widehat{u})^2\right\rangle_\rho + \left\langle(\Delta\widehat{v})^2\right\rangle_\rho = \sum_i p_i\left(\left\langle\widehat{u}^2\right\rangle_i + \left\langle\widehat{v}^2\right\rangle_i\right) - \langle\widehat{u}\rangle_\rho^2 - \langle\widehat{v}\rangle_\rho^2 \\
= &\sum_i p_i\left(\left\langle(t_1|\alpha|\sin((\hat{n}_2 - t_2^2|\beta|^2)\theta))^2\right\rangle_i + \left\langle(t_2|\beta|\sin((\hat{n}_1 - t_1^2|\alpha|^2)\theta))^2\right\rangle_i + \left\langle\widehat{p}_1^2\right\rangle_i + \left\langle\widehat{p}_2^2\right\rangle_i\right) \\
&+2\left(\sum_i p_i\left\langle(t_1|\alpha|\sin((\hat{n}_2 - t_2^2|\beta|^2)\theta))^2\right\rangle_i\langle\widehat{p}_1\rangle_i - \sum_i p_i\left\langle\left\langle(t_2|\beta|\sin((\hat{n}_1 - t_1^2|\alpha|^2)\theta))^2\right\rangle\right\rangle_i\langle\widehat{p}_2\rangle_i\right) \\
&-\langle\widehat{u}\rangle_\rho^2 - \langle\widehat{v}\rangle_\rho^2 \\
= &\sum_i p_i\left(\left\langle\left(\Delta t_1|\alpha|\sin((\hat{n}_2 - t_2^2|\beta|^2)\theta)\right)^2\right\rangle_i + \left\langle(\Delta\widehat{p}_1)^2\right\rangle_i + \left\langle\left(\Delta t_2|\beta|\sin((\hat{n}_1 - t_1^2|\alpha|^2)\theta)\right)^2\right\rangle_i + \left\langle(\Delta\widehat{p}_2)^2\right\rangle_i\right) \\
&+\sum_i p_i\langle\widehat{u}\rangle_i^2 - \left(\sum_i p_i\langle\widehat{u}\rangle_i\right)^2 + \sum_i p_i\langle\widehat{v}\rangle_i^2 - \left(\sum_i p_i\langle\widehat{v}\rangle_i\right)^2 \\
\geq &\sum_i p_i\left(\left\langle\left(\Delta t_1|\alpha|\sin((\hat{n}_2 - t_2^2|\beta|^2)\theta)\right)^2\right\rangle_i + \left\langle(\Delta\widehat{p}_1)^2\right\rangle_i + \left\langle\left(\Delta t_2|\beta|\sin((\hat{n}_1 - t_1^2|\alpha|^2)\theta)\right)^2\right\rangle_i + \left\langle(\Delta\widehat{p}_2)^2\right\rangle_i\right) \\
\geq &\left|\left\langle\left[\hat{p}_1, t_2|\beta|\sin((\hat{n}_1 - t_1^2|\alpha|^2)\theta)\right]\right\rangle\right| + \left|\left\langle\left[\hat{p}_2, t_1|\alpha|\sin((\hat{n}_2 - t_2^2|\beta|^2)\theta)\right]\right\rangle\right|.
\end{aligned}$$

Here the symbol $\langle\cdots\rangle_i$ denotes average over the product density operator $\rho_{i1}\otimes\rho_{i2}$. We have used the Cauchy-Schwarz inequality $\left(\sum_i p_i\right)\left(\sum_i p_i\langle\widehat{u}\rangle_i^2\right) \geq \left(\sum_i p_i|\langle\widehat{u}\rangle_i|\right)^2$ and the uncertainty relation that $\left\langle\left(\Delta\widehat{A}_j\right)^2\right\rangle_i + \left\langle\left(\Delta\widehat{B}_j\right)^2\right\rangle_i \geq \left|\left[\widehat{A}_j, \widehat{B}_j\right]\right|$ for $j = 1, 2$.

We thus define the entanglement witness as follow,

$$W = Log_2 \frac{|\langle[\hat{p}_1, t_2|\beta| \sin((\hat{n}_1 - t_1^2|\alpha|^2)\theta)]\rangle| + |\langle[\hat{p}_2, t_1|\alpha| \sin((\hat{n}_2 - t_2^2|\beta|^2)\theta)]\rangle|}{(\Delta\hat{u})^2 + (\Delta\hat{v})^2} \tag{5.15}$$

5.4.3 Calculation of the value of the witness under decoherence

The state with loss is

$$\begin{aligned} |\psi\rangle &= \sum_{m,k=0}^{\infty} |t_1\alpha e^{-i(m+k)\theta}\rangle_1 |r_1\alpha e^{-i(m+k)\theta}\rangle_3 e^{-\frac{|\beta|^2}{2}} \frac{(t_2\beta)^m}{\sqrt{m!}} |m\rangle_2 \frac{(r_2\beta)^k}{\sqrt{k!}} |k\rangle_4 \\ &= \sum_{m,k=0}^{\infty} |t_2\beta e^{-i(m+k)\theta}\rangle_1 |r_2\beta e^{-i(m+k)\theta}\rangle_3 e^{-\frac{|\alpha|^2}{2}} \frac{(t_1\alpha)^m}{\sqrt{m!}} |m\rangle_2 \frac{(r_1\alpha)^k}{\sqrt{k!}} |k\rangle_4 \end{aligned}$$

$$\begin{aligned} \hat{u} &= \hat{p}_1 + t_1|\alpha| \sin((\hat{n}_2 - t_2^2|\beta|^2)\theta) \\ \hat{v} &= \hat{p}_2 + t_2|\beta| \sin((\hat{n}_1 - t_1^2|\alpha|^2)\theta) \end{aligned}$$

We first calculate the variance $\left\langle (\Delta\widehat{u})^2 \right\rangle = \langle \widehat{u}^2 \rangle - \langle \widehat{u} \rangle^2$

$$\begin{aligned} \langle \widehat{u} \rangle^2 &= (e^{-|\beta|^2} \sum_{m,k=0}^{\infty} \frac{(t_2\beta)^{2m}}{m!} \frac{(r_2\beta)^{2k}}{k!} (\langle t_1\alpha e^{-i(m+k)\theta} | \hat{p_1} | t_1\alpha e^{-i(m+k)\theta} \rangle + \left\langle m | t_1|\alpha| \sin((\hat{n}_2 - t_2^2|\beta|^2)\theta) | m \right\rangle))^2 \\ &= (e^{-|\beta|^2} \sum_{m,k=0}^{\infty} \frac{(t_2\beta)^{2m}}{m!} \frac{(r_2\beta)^{2k}}{k!} (t_1|\alpha| \sin((|\beta|^2 - m - k)\theta) + t_1|\alpha| \sin((m - t_2^2|\beta|^2)\theta)))^2 \end{aligned}$$

$$\begin{aligned} \left\langle \widehat{u}^2 \right\rangle &= \left\langle \widehat{p}_1^2 + 2\widehat{p}_1 t_1|\alpha| \sin((\hat{n}_2 - t^2b^2)\theta) + (t_1|\alpha|)^2 \sin^2((\hat{n}_2 - t_2^2|\beta|^2)\theta) \right\rangle \\ &= e^{-|\beta|^2} \sum_{m,k=0}^{\infty} \frac{(t_2\beta)^{2m}}{m!} \frac{(r_2\beta)^{2k}}{k!} (\langle t_1\alpha e^{-i(m+k)\theta} | \widehat{p}_1^2 | t_1\alpha e^{-i(m+k)\theta} \rangle \\ &\quad +2t_1|\alpha| \sin((|\beta|^2 - m - k)\theta) t_1|\alpha| \sin((m - t_2^2|\beta|^2)\theta) + (t_1|\alpha|)^2 \sin^2((m_2 - t_2^2|\beta|^2)\theta)) \\ &= e^{-|\beta|^2} \sum_{m,k=0}^{\infty} \frac{(t_2\beta)^{2m}}{m!} \frac{(r_2\beta)^{2k}}{k!} (\langle t_1\alpha e^{-i(m+k)\theta} | \frac{(\hat{a_1} - \hat{a_1}^\dagger)(\hat{a_1} - \hat{a_1}^\dagger)}{-4} | t_1\alpha e^{-i(m+k)\theta} \rangle \\ &\quad +2t_1|\alpha| \sin((|\beta|^2 - m - k)\theta) t_1|\alpha| \sin((m - t_2^2|\beta|^2)\theta) + (t_1|\alpha|)^2 \sin^2((m_2 - t_2^2|\beta|^2)\theta)) \\ &= e^{-|\beta|^2} \sum_{m,k=0}^{\infty} \frac{(t_2\beta)^{2m}}{m!} \frac{(r_2\beta)^{2k}}{k!} (\langle t_1\alpha e^{-i(m+k)\theta} | \frac{\hat{a_1}^2 + (\hat{a_1}^\dagger)^2 - 2\hat{a_1}^\dagger \hat{a_1} - 1)}{-4} | t_1\alpha e^{-i(m+k)\theta} \rangle \\ &\quad +2t_1|\alpha| \sin((|\beta|^2 - m - k)\theta) t_1|\alpha| \sin((m - t_2^2|\beta|^2)\theta) + (t_1|\alpha|)^2 \sin^2((m - t_2^2|\beta|^2)\theta)) \end{aligned}$$

$$
\begin{aligned}
&= e^{-|\beta|^2}\sum_{m,k=0}^{\infty}\frac{(t_2\beta)^{2m}}{m!}\frac{(r_2\beta)^{2k}}{k!}((t_1|\alpha|\sin((|\beta|^2-m-k)\theta))^2+\frac{1}{4}\\
&\quad +2t_1|\alpha|\sin((|\beta|^2-m-k)\theta)t_1|\alpha|\sin((m-t_2^2|\beta|^2)\theta)+(t_1|\alpha|)^2\sin^2((m-t_2^2|\beta|^2)\theta))\\
&= \frac{1}{4}+(t_1|\alpha|)^2e^{-|\beta|^2}\sum_{m,k=0}^{\infty}\frac{(t_2\beta)^{2m}}{m!}\frac{(r_2\beta)^{2k}}{k!}((\sin((|\beta|^2-m-k)\theta))+\sin((m-t_2^2|\beta|^2)\theta)^2)
\end{aligned}
$$

Similar results holds for $\hat{v}$.

To calculate the average of the commutator $|\langle[\hat{p}_1,t_2|\beta|\sin((\hat{n}_1-t_1^2|\alpha|^2)\theta)]\rangle|$,

$$
\begin{aligned}
&\left|\left\langle\left[\hat{p}_1,t_2|\beta|\sin((\hat{n}_1-t_1^2|\alpha|^2)\theta)\right]\right\rangle\right|\\
&= |\left\langle\hat{p}_1t_2|\beta|\sin((\hat{n}_1-t_1^2|\alpha|^2)\theta)-t_2|\beta|\sin((\hat{n}_1-t_1^2|\alpha|^2)\theta)\hat{p}_1\right\rangle|\\
&= |e^{-|\beta|^2}\sum_{m,k=0}^{\infty}\frac{(t_2\beta)^{2m}}{m!}\frac{(r_2\beta)^{2k}}{k!}(\langle t_1\alpha e^{-i(m+k)\theta}|\frac{\hat{a_1}-\hat{a_1}^\dagger}{2i}t_2|\beta|\sin((\hat{n}_1-t_1^2|\alpha|^2)\theta)\\
&\quad -t_2|\beta|\sin((\hat{n}_1-t_1^2|\alpha|^2)\theta)\frac{\hat{a_1}-\hat{a_1}^\dagger}{2i}|t_1\alpha e^{-i(m+k)\theta}\rangle|
\end{aligned}
$$

$$
\begin{aligned}
&\langle t_1\alpha e^{-i(m+k)\theta}|\hat{a_1}t_2|\beta|\sin((\hat{n}_1-t_1^2|\alpha|^2)\theta)|t_1\alpha e^{-i(m+k)\theta}\rangle\\
&= t_2|\beta|\langle t_1\alpha e^{-i(m+k)\theta}|\hat{a_1}\sin((n-t_1^2|\alpha|^2)\theta)e^{-\frac{|t_1\alpha|^2}{2}}\sum_{n=0}^{\infty}\frac{(t_1\alpha)^{2n}}{n!}|n\rangle\\
&= t_2|\beta|e^{-\frac{|t_1\alpha|^2}{2}}\sum_{n=0}^{\infty}\frac{(t_1\alpha e^{-i(m+k)\theta})^{2n}}{\sqrt{n!}}\sin((n-t_1^2|\alpha|^2)\theta)\langle t_1\alpha e^{-i(m+k)\theta}|\hat{a_1}|n\rangle\\
&= t_2|\beta|e^{-\frac{|t_1\alpha|^2}{2}}\sum_{n=0}^{\infty}\frac{(t_1\alpha e^{-i(m+k)\theta})^{2n}}{\sqrt{n!}}\sin((n-t_1^2|\alpha|^2)\theta)\langle t_1\alpha e^{-i(m+k)\theta}|\sqrt{n}|n-1\rangle\\
&= t_2|\beta|e^{-\frac{|t_1\alpha|^2}{2}}\sum_{n=0}^{\infty}\frac{(t_1\alpha e^{-i(m+k)\theta})^{2n}}{\sqrt{n!}}\sin((n-t_1^2|\alpha|^2)\theta)e^{-\frac{|t_1\alpha|^2}{2}}\sum_{n=0}^{\infty}\frac{(t_1\alpha^\star e^{i(m+k)\theta})^{2l}}{\sqrt{l!}}\langle l|\sqrt{n}|n-1\rangle\\
&= t_2t_1|\beta|\alpha e^{-i(m+k)\theta}e^{-|t_1\alpha|^2}\sum_{n=0}^{\infty}\frac{|t_1\alpha|^{2n}}{n!}\sin((n-t_1^2|\alpha|^2)\theta)
\end{aligned}
$$

For similar reasons,

$$
\begin{aligned}
&\langle t_1\alpha e^{-i(m+k)\theta}|\hat{a_1}^\dagger t_2|\beta|\sin((\hat{n}_1-t_1^2|\alpha|^2)\theta)|t_1\alpha e^{-i(m+k)\theta}\rangle\\
&= t_2t_1|\beta|\alpha^\star e^{i(m+k)\theta}e^{-|t_1\alpha|^2}\sum_{n=0}^{\infty}\frac{|t_1\alpha|^{2n}}{n!}\sin((n-t_1^2|\alpha|^2)\theta)
\end{aligned}
$$

$$
\begin{aligned}
& \langle t_1\alpha e^{-i(m+k)\theta}|t_2|\beta|\sin((\hat{n}_1 - t_1^2|\alpha|^2)\theta)\hat{a_1}|t_1\alpha e^{-i(m+k)\theta}\rangle \\
= \;& t_2 t_1|\beta|\alpha e^{-i(m+k)\theta} e^{-|t_1\alpha|^2} \sum_{n=0}^{\infty} \frac{|t_1\alpha|^{2n}}{n!} \sin((n+1-t_1^2|\alpha|^2)\theta)
\end{aligned}
$$

$$
\begin{aligned}
& \langle t_1\alpha e^{-i(m+k)\theta}|t_2|\beta|\sin((\hat{n}_1 - t_1^2|\alpha|^2)\theta)\hat{a_1}^{\dagger}|t_1\alpha e^{-i(m+k)\theta}\rangle \\
= \;& t_2 t_1|\beta|\alpha^{\star} e^{i(m+k)\theta} e^{-|t_1\alpha|^2} \sum_{n=0}^{\infty} \frac{|t_1\alpha|^{2n}}{n!} \sin((n+1-t_1^2|\alpha|^2)\theta)
\end{aligned}
$$

Thus we have

$$
\begin{aligned}
& \left|\left\langle \left[\hat{p}_1, t_2|\beta|\sin((\hat{n}_1 - t_1^2|\alpha|^2)\theta)\right]\right\rangle\right| \\
= \;& t_2 t_1|\beta||\alpha||e^{-|\beta|^2} \sum_{m,k=0}^{\infty} \frac{(t_2\beta)^{2m}}{m!}\frac{(r_2\beta)^{2k}}{k!}\cos((|\beta|^2 - m + k)\theta) \\
& * e^{-|t_1\alpha|^2} \sum_{n=0}^{\infty} \frac{|t_1\alpha|^{2n}}{n!}(\sin((n+1-t_1^2|\alpha|^2)\theta) - \sin((n-t_1^2|\alpha|^2)\theta))
\end{aligned}
$$

Bibliography

[1] Mario Krenn, Marcus Huber, Robert Fickler, Radek Lapkiewicz, Sven Ramelow, Anton Zeilinger, PNAS 111(17), 6243-6247 (2014).

[2] A. I. Lvovsky, R. Ghobadi, A. Chandra, A. S. Prasad, and C. Simon, Nature Physics 9, 541 (2013), 00007.

[3] N. Bruno, A. Martin, P. Sekatski, N. Sangouard, R. T. Thew, and N. Gi\\sin, Nature Physics 9, 545 (2013), 00011.

[4] W. Marshall, C. Simon, R. Penrose, and D. Bouwmeester, Physical Review Letters 91, 130401 (2003), 00545.

[5] M. Aspelmeyer, T. J. Kippenberg, and F. Marquardt, arXiv:1303.0733 [cond-mat, physics:quant-ph] (2013).

[6] G. Kirchmair, B. Vlastakis, Z. Leghtas, S. E. Nigg, H. Paik, E. Ginossar, M. Mirrahimi, L. Frunzio, S. M. Girvin, and R. J. Schoelkopf, Nature 495, 205 (2013).

[7] B. Yurke and D. Stoler, Phys. Rev. Lett. 57, 13 (1986).

[8] H. Lau, Z. Dutton, T Wang, and C Simon, http://arxiv.org/abs/1404.1394

[9] T. Wang, R. Ghobadi, S. Raeisi, and C. Simon, Phys. Rev. A 88, 062114 (2013).

[10] Lu-Ming Duan, G. Giedke, J. I. Cirac, and P. Zoller, PhysRevLett.84.2722

[11] V. Venkataraman, K. Saha, and A. L. Gaeta, Nature Photonics 7, 138-141 (2013).

[12] M. Weidemller, Nature Physics 5, 91 - 92 (2009)

[13] Munro, W. J., Nemoto, K. & Spiller, T. P. Weak nonlinearities: a new route to optical quantum computation. New J. Phys. 7, 137 (2005).

[14] Imoto, N., Haus, H. A. & Yamamoto, Y. Quantum nondemolition measurement of the photon number via the optical Kerr effect. Phys. Rev. A 32, 2287?2292 (1985).

[15] Spiller, T. P. et al. Quantum computation by communication. New J. Phys. 8, 30 (2006).

[16] Nemoto, K. & Munro, W. J. Nearly deterministic linear optical controlled-NOT gate. Phys. Rev. Lett. 93, 250502 (2004).

[17] Barrett, S. D. et al. Symmetry analyzer for nondestructive Bell-state detection u\\sing weak nonlinearities. Phys. Rev. A 71, 060302(R) (2005).

Chapter 6

Conclusion and outlook

This thesis mainly discusses the topic why it is hard to observe macroscopic quantum effects. We approach this topic from the quantum optics point of view, especially with the help of Kerr effects. Aside from the obvious fact that no interference experiments are done in daily experience so that quantum effect cannot be shown, we focus on two other reasons. Chapter 3 and 4 analyze the fact that coarse graining in measurement precision makes it hard to observe macroscopic quantum effects in two different aspects. Chapter 3 shows that to create macroscopic quantum effect we need a precision that scales with the size of the system. Chapter 4 shows that even if we have a perfect macroscopic quantum state, the measurement resolution required to observe it scales with the size of the system, when both outcome and control precision are taken into consideration. Chapter 5 tackles the problem of decoherence, a major obstacle preventing us from creating and observing macroscopic quantum effects. We propose to create and detect strong macroscopic entanglement via small Kerr phase shift, which is robust under decoherence. We hope that the above results are helpful to push the boundary of the realm of quantum theory to the macroscopic level.

In my opinion, there are several directions for future studies about the topic of macroscopic quantum effects.

The first one is how to define macroscopic quantum effects itself, especially macroscopic entanglement. Intuitively, there could be several criteria of macroscopicity [1, 2, 3, 4, 5]. Firstly, the size of the state is large, such as a large coherent states with different phases as given in the examples of Chapter 3, 4 and 5 and different states of mirrors in optomechanical system, or even living and dead cats. Secondly, the amount of entanglement is large. This is in some sense equivalent to that the dimension of entanglement is large. The

state analyzed in Chapter 5 is just a good example. Thirdly, the number of particles involved in the entanglements is large, for instance, a complicated cluster states with a great amount of qubits. There is another class of large entanglement, the status of which is ambiguous. Consider sending a single excitation into some medium, for example, sending a photon into BEC, creating a spinwave. The BEC, a macroscopic system, is in a superposition of different states, with the excitation in any of the atoms. Shall we consider this as a macroscopic quantum effect? I would prefer not. In my opinion, a macroscopic effect should have a large number of excitations, as in previous three classes discussed above.

A natural question would be, how to develop a quantitative measurement that is applicable to the above three macroscopic states? In Chapter 5, the states we proposed are macroscopic satisfying both the first and second criterion above. We used logarithmic negativity to quantify the entanglement, which obviously scales with both the size of the system and the amount of entanglement. However, when the size of the system becomes large, the computation power needed would be enormous. And the logarithmic negativity could not be applied to the third criterion. So the question of quantitative measurement of macroscopicity still open.

Another direction is about the topic of precision requirement to observe macroscopic quantum effects. In Chapter 4 we conjectured that the measurement precision required for demonstrating macroscopic quantum effects seems to increase with the size of the system, provided that both outcome precision and control precision are taken into account. The next problem would be how to quantitatively describe the complimentary relationship of the outcome precision and control precision. For example, we can try to find a system and analyze if we decrease a certain amount of outcome precision, how much more control precision is needed. Moreover, how to really prove the above conjecture is also an interesting problem.

The third direction is about creating and detecting macroscopic entanglement that is ro-

bust under decoherence. In chapter 5 we proposed a method to create such states, showing that the entanglement is robust under decoherence. However, although we can in principle quantify the entanglement by logarithmic negativity, the computational resource required when the size of the system is very large is tremendous. A natural question is, if there some better way to quantify this entanglement. Moreover, we propose to detect such entanglement via homodyne tomography, but when the size of the system goes really large, such tomography may be hard to realize. So another question is, are there some other ways to detect such macroscopic entanglement?

Above are some interesting questions for future studies. We hope that the realm of quantum theory can be further pushed towards the macroscopic level by these endeavors.

Bibliography

[1] Leggett, A. J., J. Phys. Condens. Matter 14, R415 (2002).

[2] Dur, W., Simon, C. Cirac, J. I., Phys. Rev. Lett. 89, 210402 (2002).

[3] Sekatski, P. et al., Phys. Rev. A 86, 060301(R) (2012).

[4] Raeisi, S., Tittel, W. Simon, C., Phys. Rev. Lett. 108, 120404 (2012).

[5] Pavel Sekatski, Nicolas Gisin, Nicolas Sangouard, arXiv:1402.2542